

Disorder-quenched Kondo effect in mesoscopic electronic systems

Stefan Kettemann¹ and Eduardo R. Mucciolo²

¹ *Institut für Theoretische Physik, Universität Hamburg, Jungiusstraße 9, 20355 Hamburg, Germany, and*

² *Department of Physics, University of Central Florida, P.O. Box 162385, Orlando, FL 32816-2385, USA*

(Dated: September 26, 2018)

Nonmagnetic disorder is shown to quench the screening of magnetic moments in metals, the Kondo effect. The probability that a magnetic moment remains free down to zero temperature is found to increase with disorder strength. Experimental consequences for disordered metals are studied. In particular, it is shown that the presence of magnetic impurities with a small Kondo temperature enhances the electron's dephasing rate at low temperatures in comparison to the clean metal case. It is furthermore proven that the width of the distribution of Kondo temperatures remains finite in the thermodynamic (infinite volume) limit due to wave function correlations within an energy interval of order $1/\tau$, where τ is the elastic scattering time. When time-reversal symmetry is broken either by applying a magnetic field or by increasing the concentration of magnetic impurities, the distribution of Kondo temperatures becomes narrower.

PACS numbers: 72.10.Fk, 72.15.-m, 75.20.Hr

Keywords: Kondo effect, Anderson localization, phase coherence

I. INTRODUCTION

A local magnetic impurity changes the ground state of a Fermi liquid due to the correlations created by the antiferromagnetic exchange interaction between its localized spin and the delocalized electrons.^{1,2} At temperatures below the Kondo temperature T_K the spin of the magnetic impurity is screened by the formation of a singlet state with the conduction electrons.^{3,4} Disorder affects the formation of this Kondo singlet in various ways.⁵ In particular, the Kondo temperature may depend on the positioning of the magnetic impurities in the host lattice. Thus, for a sample containing many magnetic impurities, T_K may be distributed due to fluctuations of the microscopic exchange coupling.^{6,7,8} Impurities (magnetic or nonmagnetic) and lattice defects also cause fluctuations in the local density of states (LDOS) of the conduction electrons at the magnetic impurity site. Thus, the distributions of the Kondo temperature and of the LDOS are related in a disordered metal.^{9,10}

In this paper we explore the consequences of nonmagnetic disorder for the Kondo effect. We base our study on the statistical properties of T_K for the different dynamical regimes of a disordered metal. Note that the Kondo temperature accounts for a crossover rather than a sharp transition in the metal properties and that may raise the question whether T_K is sufficiently well defined. In weakly disordered metals it is possible in principle to extract T_K by fitting physical quantities such as the spin susceptibility and the electron dephasing rate versus temperature against the corresponding universal scaling function. While that scaling function may be modified itself by the disorder,^{8,11} the Kondo screening is still governed by T_K , and one may study its sample-to-sample fluctuations. Below, we show that these fluctuations may have a significant impact on the low-temperature properties of a metallic sample even in the thermodynamic, infinite volume limit.

It is useful to compare the magnitude of T_K to other relevant energy scales of a metallic sample. These scales are the mean level spacing $\Delta = 1/\nu L^d$, the Thouless energy $E_c = D_e/L^2$, and the elastic scattering rate $1/\tau$. Here, ν

denotes the density of states at the Fermi level, $D_e = v_F^2 \tau / d$ is the diffusion constant, and d is the dimensionality of diffusion (we have set $\hbar = k_B = 1$). This comparison allows one to establish several distinct regimes, as sketched in Fig. 1. We note that, in practice, T_K does not exceed $1/\tau$ in metals, therefore standard perturbation theory in the disorder potential may not be used to describe the effect of disorder on the Kondo effect. However, there is a large regime of experimental interest where a diagrammatic expansion may be used, namely, $E_c < T_K < 1/\tau$.¹² For small samples, when $\Delta < T_K < E_c$, random matrix theory (RMT) can be applied and the distribution of Kondo temperatures is expected to scale with Δ alone. In the opposite limit, when the sample is so large that the localization length ξ is smaller than the linear size L , the Thouless energy and the global level spacing are irrelevant and the Kondo temperature is determined by the mean level spacing for states localized in the vicinity of the magnetic impurity, $\Delta_\xi = 1/\nu \xi^d$.^{13,14,15} In this case, one can expect the distribution of Kondo temperatures to scale with Δ_ξ instead of Δ . Finally, when T_K is smaller than the spacing between neighboring energy levels at the Fermi surface (either Δ or Δ_ξ), the distribution of T_K will be mainly determined by the fluctuations of the wave functions and level spacing of the two eigenstates closest to the Fermi energy. Accordingly, in this regime the Kondo temperature is determined by the coupling of the magnetic impurity to a two-level system (2LS).

Our analytical calculations show that the average Kondo temperature is enhanced by weak disorder. Disorder also induces a *finite width* in the distribution of T_K which is shown to persist even in the infinite sample, thermodynamic limit. This effect is due to the existence of local correlations between eigenfunctions at different energies within a macroscopically large energy interval $1/\tau$. These spectral correlations also lead to a bimodal structure in the distribution of T_K , with a long tail stretching toward $T_K = 0$. The numerical simulations show that for a sizeable number of disorder configurations, no finite value of T_K exist within the lowest order self-consistent perturbation theory, indicating that in those cases the magnetic moment is not screened by the conduction elec-

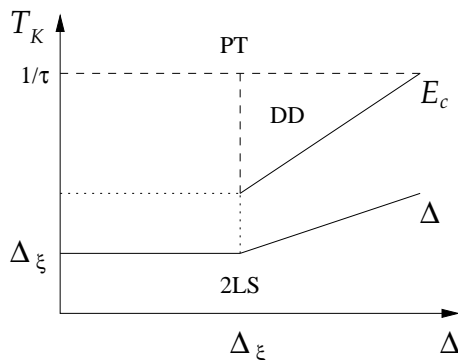


FIG. 1: Overview of the different regimes of a mesoscopic Kondo system of linear size L , as parametrized by the system's mean level spacing $\Delta = 1/\nu L^d$ and the unaveraged Kondo temperature of a single magnetic impurity T_K . E_c is the Thouless energy, $1/\tau$ is the elastic scattering rate, and $\Delta_\xi = 1/\nu \xi^d$, with ξ being the localization length. The acronyms denote: Two levels coupled to the magnetic impurity (2LS), diagrammatic expansion in diffusion ladder diagrams (DD), and perturbative regime (PT), with $1/g = (E_F \tau)^{-1}$ as the small expansion parameter. We only consider metallic systems where the relation $\Delta_\xi \ll 1/\tau \ll E_F$ is fulfilled.

trons. We find that there is a finite probability of having free moments even for values of J such that the average Kondo temperature $\langle T_K \rangle$ is much larger than the mean level spacing Δ .

For small metallic grains, it is well-known that RMT provides a very good description of the statistical fluctuations of single-particle states. We therefore use RMT to investigate analytically and numerically the statistics of T_K in such systems. The ratio between the standard deviations of T_K for the orthogonal and unitary ensemble is found numerically to be equal to $\sqrt{2}$ for a wide range of exchange couplings J , in agreement with analytical calculations. Furthermore, it is shown numerically that a finite number of free moments persists to exist in this regime. This result is consistent with an analytical calculation based on the 2LS approximation.

In regard to the width of the distribution of T_K in the RMT regime, we find a counter-intuitive result at first glance, namely, that the distribution becomes *narrower* when increasing the concentration. This effect maybe understood as a consequence of the suppression of the weak localization correction by the breaking of time-reversal invariance, which in RMT is seen as a reduction in wave function fluctuations. We also consider whether additional correlations between wave functions induced by breaking of time-reversal symmetry¹⁶ within an interval of order of the spin scattering rate $1/\tau_s$ can lead to an enhancement of the width of the distribution of T_K . We find that while the width increases by a factor $\sqrt{T_K \tau_s}$ as compared to the pure RMT ensembles, it nevertheless vanishes in the thermodynamic limit when $\Delta \rightarrow 0$, and therefore is negligible in comparison with the magnitude of the broadening caused by wave functions correlations beyond RMT.

The large fluctuations of T_K in disordered metals impact the behavior of several thermodynamic and transport properties at low temperatures. We consider in particular the influ-

ence of these fluctuations on the temperature dependence of the electron's dephasing rate. We find that nonmagnetic disorder combined with spin scattering due to magnetic impurities increases the dephasing rate at temperatures $T < \langle T_K \rangle$. The dephasing rate is readily accessible in transport experiments by measuring weak-localization corrections to the resistance. Our predictions are in qualitative agreement with recent experimental results.

Our work details and extends the discussions provided in a previous letter (Ref. 10) and also includes new numerical and analytical results. The presentation is organized in the following way. In Sec. II we introduce the problem of finding the distribution of the Kondo temperature as defined by an integral equation. The central analytical and numerical results of our paper are presented in Secs. III and IV, respectively. There, the distribution, average, and standard deviation of the Kondo temperature are studied as function of disorder strength by taking eigenstates and eigenenergies from a disordered tight-binding model. The average and standard deviation are derived analytically as function of Δ , E_c , and the disorder strength and compared with the numerical results. We also study how the number of free moments depends on the exchange coupling and disorder strength.

In Sec. VI, we consider the RMT regime. We present the analytical results obtained for the distribution of T_K by taking into account only wave function fluctuations. We compare analytical estimates of the average and standard deviation of T_K with numerical results obtained from simulations of random matrix ensembles. Both large- and small- T_K limit are considered.

The dependence of the distribution of the Kondo temperature on the concentration of magnetic impurities is studied in Sec. VII. In Sec. VIII we describe how the fluctuations of T_K affect the dephasing time of electrons in metallic thin films and quasi-one-dimensional wires. Finally, in Sec. IX we summarize our results and make our concluding remarks. Appendix A includes the derivation of the integral equation for the Kondo temperature in a one-loop approximation for a disordered sample, together with a critical discussion of its validity. In Appendix B, for reference, we briefly present the solution of the integral equation in the clean limit using a picket-fence spectrum (equidistant energy levels).

II. FORMULATION OF THE PROBLEM

We will consider a single magnetic impurity in an isolated, phase-coherent metallic sample where the energy levels are well separated, a system previously referred in the literature as the Kondo box.^{17,18} To determine T_K , we will adopt the following self-consistent equation,^{10,19,20}

$$1 = \frac{J}{2N} \sum_{n=1}^N \frac{\Omega |\psi_n(0)|^2}{E_n - E_F} \tanh \left(\frac{E_n - E_F}{2T_K} \right), \quad (1)$$

where N is the number of states in the spectrum, $\Omega = L^d$ is the sample volume, E_F is the Fermi energy, and J is the exchange coupling between the magnetic impurity and the delo-

calized electrons. The eigenenergies and eigenfunctions of the sample are, respectively, E_n and $\psi_n(\mathbf{r})$, while the impurity is located at $\mathbf{r} = 0$. Equation (1) is obtained from second-order perturbation theory in Appendix A. A similar expression can be obtained from the zero-temperature, self-consistent solution of the one-loop renormalization group (RG) equation.^{4,21} However, in that case one misses the tanh factor (which accounts for the finite-temperature occupation numbers) and the result is only valid for $T_K \gg \Delta$. While the approximations involved in deriving Eq. (1) are not sufficient for describing the properties of the system below T_K , it is important to remark that Eq. (1) does yield a good estimate for the Kondo temperature, which is the relevant scale for the low-temperature behavior of Kondo systems. The two-loop correction has been found to change the Kondo temperature by a factor $\sqrt{J/D}$.⁴ In the thermodynamic limit (infinite volume), the physics at temperatures $T \ll T_K$ is known to be that of an effective Fermi liquid, where the Kondo temperature determines the Landau parameters.³ For example, the effective mass, the density of states, and thereby the specific heat become enhanced by a factor $1 + n_m/(\pi\nu T_K)$, while the paramagnetic susceptibility is enhanced by a factor $1 + 2n_m/(\pi\nu T_K)$, where n_m is the concentration of magnetic impurities.^{2,3}

It is convenient to rescale Eq. (1) to a dimensionless form, in which case it becomes

$$1 = \frac{1}{2x} \sum_{n=1}^N \frac{x_n}{s_n} \tanh\left(\frac{s_n}{2\kappa}\right), \quad (2)$$

where $x = D/J$, $\kappa = T_K/D$, $x_n = \Omega|\psi_n(\mathbf{r})|^2$ is the probability density of the n th eigenstate, and $s_n = (E_n - E_F)/\Delta$ is the corresponding eigenenergy measured relative to the Fermi energy in units of Δ . In the following, we will assume that the Fermi energy is in the middle of two energy levels, so that the number of electrons in the Kondo box is even. (For an odd number of electrons, the unpaired electron at the Fermi energy forms a singlet with the magnetic impurity with binding energy J and the problem becomes trivial.) Using Eq. (2), the distribution of Kondo temperatures is determined by

$$P(T_K) = \left| \frac{d}{dT_K} \int_0^{D/J} dx \langle \delta(x - F(T_K)) \rangle \right|, \quad (3)$$

where

$$F(T_K) = \frac{1}{2} \sum_{n=1}^N \frac{x_n}{s_n} \tanh\left(\frac{s_n}{2\kappa}\right).$$

We note that a similar expression appears in the calculation of the distribution of NMR-Knight shifts for metallic grains with a finite level width Γ .^{22,23,24} There, an exact solution of the problem was derived within RMT in the limit $N \gg 1$. However, two aspects make the problem defined by Eq. (3) much harder to solve. First, in the NMR-Knight shift case, instead of Eq. (4), the calculation involves a sum over terms which behave as $1/(s_n^2 + \Gamma^2)$, decaying faster than $1/s_n$ at large

energies. Second and more importantly, since the Kondo temperature enters in Eq. (4) essentially as the low-energy cut-off of the sum, we cannot apply the techniques used in Refs. 22,23,24 to the calculation of the distribution of Kondo temperatures. Thus, the derivation of an exact, closed expression for the $P(T_K)$ is very nontrivial, even in RMT.

In RMT, for $\langle T_K \rangle \gg \Delta$, one would expect the distribution of Kondo temperatures to be close to a Gaussian. The reasoning behind that is the following. In this limit one can go back to Eq. (2), expand the tanh factor and find that T_K is given approximately by a sum of random variables (the wave function amplitudes). The central-limit theorem then ensures that a Gaussian distributed variable results from summing over independent random variables. However, as we show below, even for large $\langle T_K \rangle$ one finds a non-Gaussian behavior at the tails of the distribution. This feature is enhanced when considering disorder effects beyond RMT due to the appearance of local correlations between wave functions at different energies. It is therefore clear that in order to obtain the correct distribution of the Kondo temperature in disordered metals, it is crucial to abandon the assumption of independent random wave functions in Eq. (2). The main effect of wave function correlations is to broaden the distribution of T_K . This broadening survives the large-volume limit. In Sec. IV we show that correlations also induce a bimodal structure in the distribution. This should be compared with the rather featureless distribution obtained when one uses uncorrelated RMT wave functions amplitudes to evaluate T_K .¹⁰

For reference, the behavior of the Kondo temperature in the clean limit is discussed in Appendix B.

III. FLUCTUATIONS OF T_K IN A DISORDERED METAL

The effect of nonmagnetic disorder on the statistical fluctuations of the Kondo temperature is a difficult problem to study analytically. However, in the weak-disorder limit it is possible to derive expressions for the average and standard deviations of T_K *beyond RMT* by taking explicitly into account wave function correlations. To this end, we recall that the LDOS is defined as

$$\rho(\mathbf{r}, E) = \sum_{n=1}^N |\psi_n(\mathbf{r})|^2 \delta(E - E_n). \quad (4)$$

In our calculations, we will make use of the well-known correlation function of LDOS, as defined by

$$\begin{aligned} R_2(\mathbf{r}, \omega) &= \langle \rho(\mathbf{r}, E) \rho(\mathbf{r}, E + \omega) \rangle \\ &= \frac{1}{\nu^2} \sum_{n,m} \langle |\psi_n(\mathbf{r})|^2 |\psi_m(\mathbf{r})|^2 \delta(E - E_n) \\ &\quad \times \delta(E + \omega - E_m) \rangle. \end{aligned} \quad (5)$$

It is convenient to separate diagonal from off-diagonal terms in Eq. (5). The correlation function of LDOS can then be rewritten in terms of the spectral correlation function $R_2(\omega)$,

$$\begin{aligned} R_2(\mathbf{r}, \omega) &= R_2(\omega) \Omega^2 \langle |\psi_n(\mathbf{r})|^2 |\psi_m(\mathbf{r})|^2 \rangle |_{\omega=E_n-E_m} \\ &\quad + \delta(\omega/\Delta) \Omega^2 \langle |\psi_n(\mathbf{r})|^4 \rangle. \end{aligned} \quad (6)$$

Let us introduce the standard dimensionless parameter $g = E_F \tau$ to quantify the disorder strength. For $\omega < E_c$, the function $R_2(\omega)$ is an oscillatory decaying function with corrections of order $1/g^2$ to the leading RMT term. For the time-reversal symmetric case ($\beta = 1$), it reads

$$R_2\left(s = \frac{\omega}{\Delta}\right) = 1 - \frac{\sin^2(\pi s)}{\pi^2 s^2} - \left[\frac{\pi}{2} \text{sgn}(s) - \text{Si}(\pi s)\right] \left[\frac{\cos(\pi s)}{\pi s} - \frac{\sin(\pi s)}{(\pi s)^2}\right] + O(1/g^2), \quad (7)$$

where, $\text{Si}(z) = \int_0^z dy \sin y/y$.²⁵ For frequencies exceeding the Thouless energy, $\omega > E_c$, the oscillatory part of the spectral correlation function decays exponentially, while there is a correction of order $1/g^2$ which decays as $1/s$ without oscillations. While for pure RMT there are no correlations between wave functions at different energies, in systems with white-noise disorder these correlations are of order $1/g$, namely,²⁵

$$\Omega^2 \langle |\psi_n(\mathbf{r})|^2 |\psi_m(\mathbf{r})| \rangle_{\omega=E_n-E_m} = 1 + \frac{2}{\beta} \text{Re} \Pi(\omega) \quad (8)$$

for $n \neq m$, while

$$\Omega^2 \langle |\psi_n(\mathbf{r})|^4 \rangle = \left(1 + \frac{2}{\beta}\right) \left[1 + \frac{2}{\beta} \text{Re} \Pi(0)\right]. \quad (9)$$

These analytical results have recently been confirmed numerically in Ref. 26. Note that the correlation is stronger when time-reversal symmetry is present ($\beta = 1$). The dependence on the disorder enters through the summation over diffuson modes, which is here represented by

$$\Pi(\omega) = \frac{\Delta}{\pi} \sum_{\mathbf{q}} \frac{1}{D_e \mathbf{q}^2 - i\omega}. \quad (10)$$

In two dimensions (2D) and for $L > l$, one obtains²⁵

$$\Pi^{(2D)}(\omega) = \frac{1}{2\pi g} \ln \left(\frac{1/l^2 - i\omega/D_e}{1/L^2 - i\omega/D_e} \right), \quad (11)$$

with $l = v_F \tau$ and $D_e = v_F l/2$.

Since the Kondo temperature is defined by a sum over all eigenstates in the band, fluctuations of wave function amplitudes at the position of the magnetic impurity add up quite effectively when the wave functions are correlated over a large energy range. These correlations are nonzero over an interval of the order of the elastic scattering rate $1/\tau$. Thus, one can expect that fluctuations of the Kondo temperature can exist even in the thermodynamic limit, when both Δ and E_c vanish.

In order to explicitly connect the Kondo temperature to the LDOS fluctuations, we define $T_K^{(0)}$ as the Kondo temperature for a non-fluctuating LDOS, ν , and use Eq. (4) into (1) to find²⁷

$$T_K = T_K^{(0)} \exp \left[\int_{-E_F}^{D-E_F} dE \frac{\delta\rho(\mathbf{r}, E + E_F)}{2\nu E} \tanh \left(\frac{E}{2T_K} \right) \right], \quad (12)$$

where $\delta\rho \equiv \rho - \nu$. From the fact that, on average, the deviations of the local density of states vanishes, $\langle \delta\rho \rangle = 0$, and by expanding the right-hand side of Eq. (12) to second order in $\delta\rho$, we find

$$\left\langle \ln^2 \left(\frac{T_K}{T_K^{(0)}} \right) \right\rangle = \int_{-E_F}^{D-E_F} dE \int_{-E_F}^{D-E_F} dE' \times \left\langle \tanh \left(\frac{E}{2T_K^{(0)}} \right) \tanh \left(\frac{E'}{2T_K^{(0)}} \right) \times \frac{\delta\rho(\mathbf{r}, E_F + E)}{2\nu E} \frac{\delta\rho(\mathbf{r}, E_F + E')}{2\nu E'} \right\rangle. \quad (13)$$

Note that Eq. (13) provides an approximate expression for standard deviation of the Kondo temperature, δT_K : When $\delta T_K \ll \langle T_K \rangle$, we have $\delta T_K \approx T_K^{(0)} \sqrt{\langle \ln^2 (T_K/T_K^{(0)}) \rangle}$.

Using Eq. (6), the right-hand side of Eq. (13) can be broken down into three contributions, namely,

$$\left\langle \ln^2 \left(\frac{T_K}{T_K^{(0)}} \right) \right\rangle = 2 \left[S_\beta(\tau, \Delta, T_K^{(0)}) + V_\beta(\tau, E_c, T_K^{(0)}) + Q_\beta(\tau, E_c, T_K^{(0)}) \right]. \quad (14)$$

The function S_β arises from the spectral self-correlation term $\delta(\omega/\Delta)$ and is given by

$$S_\beta(\tau, \Delta, T_K) = \frac{\Delta}{8} \left(1 + \frac{2}{\beta}\right) \left[1 + \frac{2}{\beta} \text{Re} \Pi(0)\right] \times \int_{-E_F}^{D-E_F} \frac{dE}{E^2} \tanh^2 \left(\frac{E}{2T_K} \right). \quad (15)$$

This term is of order Δ/T_K and therefore vanishes in the thermodynamic limit as $\Delta \rightarrow 0$. The decaying part of the spectral correlation function yields the second term on the right-hand side of Eq. (14),

$$V_\beta(\tau, E_c, T_K) = \frac{1}{8} \int_{-E_F}^{D-E_F} \frac{dE dE'}{E E'} \tanh \left(\frac{E}{2T_K} \right) \times \tanh \left(\frac{E'}{2T_K} \right) [R_2(E - E') - 1] \times \left[1 + \frac{2}{\beta} \text{Re} \Pi(E - E')\right]. \quad (16)$$

In 2D, $R_2(\omega) - 1$ decays as $1/\omega$ for frequencies exceeding the Thouless energy. This causes V_β to be nonzero as $E_c \rightarrow 0$, but this term turns out to be only of order $1/g^2$. If correlations of wave functions are taken into account only up to first order in $1/g$, V_β can be discarded. At finite E_c , however, it needs to be taken into account since it yields terms of order E_c/T_K due to spectral correlations at small frequencies, $\omega < E_c$.

The term arising purely from the correlations of wave func-

tions is given by

$$Q_\beta(\tau, E_c, T_K) = \frac{1}{4\beta} \int \int_{-E_F}^{D-E_F} \frac{dE dE'}{E E'} \tanh\left(\frac{E}{2T_K}\right) \times \tanh\left(\frac{E'}{2T_K}\right) \text{Re} \Pi(E - E'). \quad (17)$$

This term survives the thermodynamic limit. For instance, let us consider the 2D case. From Eq. (11), we find

$$\text{Re} \Pi^{(2D)}(\omega) = \frac{1}{4\pi g} \ln\left(\frac{1/4\tau^2 + \omega^2}{E_c^2 + \omega^2}\right). \quad (18)$$

For $1/\tau \gg T_K$, one can use Eq. (18) with $E_c = 0$ to write the double integral in Eq. (17) in terms of polylogarithm functions. To leading order and after setting $E_F = D/2$, we obtain

$$Q_\beta^{(2D)}(\tau, 0, T_K) \approx \frac{1}{6\pi g \beta} \left[\ln\left(\frac{E_F}{g T_K}\right) \right]^3, \quad (19)$$

which is valid when $E_F/T_K \gg g \gg 1$. Combining Eqs. (14) and (19), we arrive at

$$\left\langle \ln^2\left(\frac{T_K}{T_K^{(0)}}\right) \right\rangle_{2D} \approx \frac{1}{3\pi g \beta} \left[\ln\left(\frac{1}{\tau T_K^{(0)}}\right) \right]^3, \quad (20)$$

which is entirely *volume independent*.

Expressions for the $\langle T_K \rangle$ and δT_K can also be derived from Eq. (13). However, in order to keep results accurate up to second order in $\delta\rho$, one has to take into account the correlation between T_K and $\delta\rho$ when expanding the right-hand side of Eq. (12). Doing so, we obtain for the average

$$\langle T_K \rangle = T_K^{(0)} \left\{ 1 + \left[1 + T_K^{(0)} \partial_{T_K^{(0)}} \right] \left[S_\beta(\tau, \Delta, T_K^{(0)}) + V_\beta(\tau, E_c, T_K^{(0)}) + Q_\beta(\tau, E_c, T_K^{(0)}) \right] \right\}. \quad (21)$$

Similarly, for the standard deviation, we arrive at

$$(\delta T_K)^2 = 2 \left(T_K^{(0)} \right)^2 \left[S_\beta(\tau, \Delta, T_K^{(0)}) + V_\beta(\tau, E_c, T_K^{(0)}) + Q_\beta(\tau, E_c, T_K^{(0)}) \right]. \quad (22)$$

Combining Eq. (20) with (22) we finally get

$$\delta T_K|_{2D} \approx T_K^{(0)} \frac{1}{\sqrt{3\pi g \beta}} \left[\ln\left(\frac{1}{\tau T_K^{(0)}}\right) \right]^{3/2}. \quad (23)$$

This expression shows that even in the weak-disorder metallic regime ($g \gg 1$) the width of the distribution of Kondo temperatures remains finite as Δ and E_c go to zero. It is interesting to note that this width is reduced by a factor $1/\sqrt{2}$ when time-reversal symmetry is broken ($\beta = 2$). This effect can be understood if we recall that the weak-localization corrections, which account for exactly half of the wave function correlation correction, become suppressed when time-reversal symmetry is fully broken. Then, only wave function correlations due to the classical diffusion propagator remain.

It is also important to remark that Eq. (23) is valid despite the fact that all electron states have a finite localization length ξ in dimensions not exceeding two. In particular, we note that the width Eq. (23) exceeds previous estimates, such as $\delta T_K \sim \sqrt{\Delta_\xi T_K^{(0)}}$, which were based on the application of RMT on the scale of the local level spacing Δ_ξ and disregarded the dominant effect of wave function correlations that we consider here.^{28,29}

From Eqs. (20) and (21), in the limit $1/\tau \gg T_K$, the average Kondo temperature is found to increase with the disorder strength as

$$\langle T_K \rangle_{2D} \approx T_K^{(0)} \left\{ 1 + \frac{1}{6\pi g \beta} \left[\ln\left(\frac{1}{\tau T_K^{(0)}}\right) \right]^3 \right\}. \quad (24)$$

Although the disorder-induced term in Eq. (24) is only of order $1/g$, it is enhanced by the large factor coming from the third power of the logarithm of $T_K^{(0)}\tau$.

These calculations can be repeated using the diffusion propagator for quasi-one-dimensional (Q1D) wires. For open boundary conditions, the diffusion propagator in Eq. (10) becomes

$$\text{Re} \Pi^{(Q1D)}(\omega) = \begin{cases} L/(k_F^2 l A), & \omega \ll E_c \\ \sqrt{6}/(k_F^2 A \sqrt{\tau \omega}), & E_c < \omega < 1/\tau, \\ 0, & \omega \gg 1/\tau, \end{cases} \quad (25)$$

where L is the length and A is the cross sectional area of the quasi-1D wire. Therefore, in the long-wire limit, with $E_c \ll T_K \ll 1/\tau$, we find

$$\left\langle \ln^2\left(\frac{T_K}{T_K^{(0)}}\right) \right\rangle_{Q1D} = \frac{4\pi\sqrt{3}}{\beta} \frac{1}{k_F^2 A} \frac{1}{\sqrt{\tau T_K^{(0)}}}, \quad (26)$$

independently of the position of the Fermi energy. Hence, the average Kondo temperature increases with disorder by an inverse square root term,

$$\langle T_K \rangle_{Q1D} \approx T_K^{(0)} \left(1 + \frac{\pi\sqrt{3}}{\beta} \frac{1}{k_F^2 A} \frac{1}{\sqrt{\tau T_K^{(0)}}} \right), \quad (27)$$

while the variance is nonvanishing by the square root of the same factor,

$$\delta T_K|_{Q1D} \approx T_K^{(0)} \sqrt{\frac{4\pi\sqrt{3}}{\beta} \frac{1}{k_F^2 A} \frac{1}{\sqrt{\tau T_K^{(0)}}}}. \quad (28)$$

The latter result is in agreement with the $1/g^{1/4}$ dependence reported in Ref. 31, where the asymptotic behavior for the 2D case, $(J^3/g)^{1/2}$, Eq. (23) was also found.

IV. NUMERICAL STUDIES OF A DISORDERED MODEL

The analytical results presented in Sec. III are applicable only in the weak-disorder regime and only predict the behavior of the two lowest moments of the distribution of Kondo

temperatures. In order to study more thoroughly the statistical fluctuations of the Kondo temperature, as well as to check the accuracy of Eqs. (21), (22), (27), and (28), we have carried out numerical studies of the fluctuations of T_K using a tight-binding model with nearest-neighbor hopping and random site potential to describe the conduction electrons. The model Hamiltonian reads

$$H = -t \sum_{\langle ij \rangle} (c_i^\dagger c_j + \text{h.c.}) + \sum_{i=1}^N V_i c_i^\dagger c_i, \quad (29)$$

where each site potential V_i is drawn from a flat box distribution of width W centered at zero. We assume each eigenstate of H to be spin degenerate, therefore sums over spins are implicit in Eq. (29). We consider only square lattices. Aspect ratios and boundary conditions are as follows: To simulate two-dimensional systems, we use a square geometry with periodic boundary conditions along both directions; For quasi-one-dimensional systems, we adopt a rectangular geometry with hard-wall (periodic) boundary conditions along the shortest (longest) length.

Employing standard numerical techniques, we have diagonalized the Hamiltonian H for a large set of realizations of the disordered potential and different lattice geometries. The resulting eigenenergies E_n and eigenvectors $\psi_n(i)$, $n = 1, \dots, N$, were used in conjunction with Eq. (1) to determine T_K . In all simulations the Fermi level was placed at the lower quarter of the band in order to avoid the large peak in the density of states at $E = 0$, reminiscent of the van Hove singularity found in the clean limit. No unfolding of energy levels was used. The simulations were carried out for 20×20 , 10×100 , and 8×200 lattice sizes, with 1,000 realizations for each value of W . In order to increase statistics, a total of 36 (20×20), 196 (10×100), and 297 (8×200) different magnetic impurity sites were used. No magnetic flux was included, thus all results refer to the time-reversal symmetric class. Partial results for the 20×20 case were previously reported in Ref. 10.

A connection between the tight-binding disorder strength W and the dimensionless parameter g (see Sec. III) can be made by recalling the expression for the nonmagnetic scattering rate in Born approximation,

$$\frac{1}{\tau} = 2\pi \nu \langle V^2 \rangle, \quad (30)$$

where $\nu = 1/\Delta L^2$ (we set the lattice constant $a = 1$, therefore $N = L^2$). Noting that $\langle V^2 \rangle = W^2/12$ and $\Delta = D/N$, we obtain

$$\frac{1}{\tau} = \frac{\pi W^2}{6 D}. \quad (31)$$

Recalling that $g = E_F \tau$ and setting $E_F = D/4$, we arrive at

$$g = \frac{3}{2\pi} \left(\frac{D}{W} \right)^2. \quad (32)$$

Equation (30) is valid only in the perturbative sense, when disorder is not too strong, and should break down near $g = 1$.

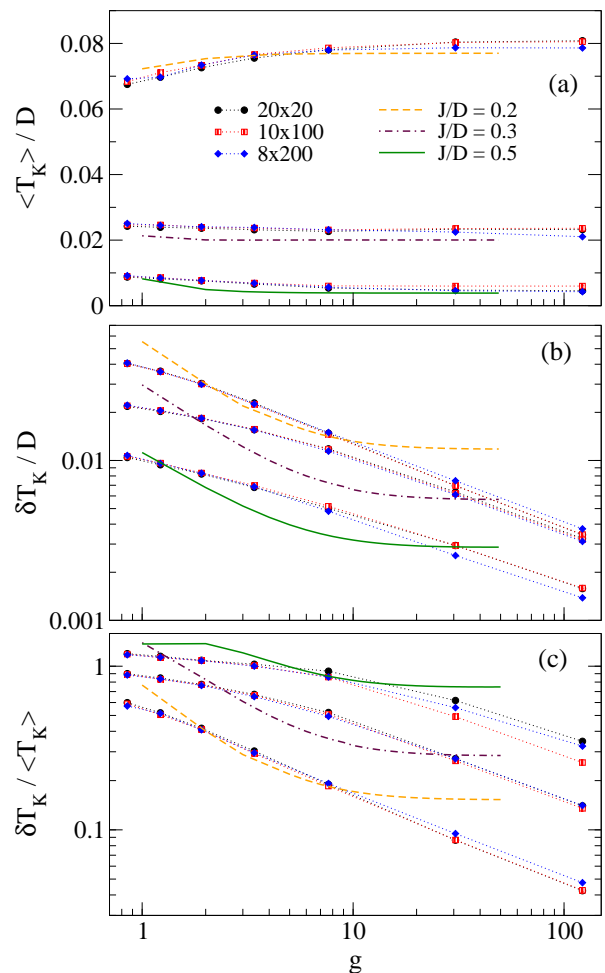


FIG. 2: (Color on-line) Average (a), standard deviation (b), and their ratio (c) as a function of disorder strength for three values of J/D and three lattice geometries: two-dimensional (20×20) and quasi-one-dimensional wires (10×100 and 8×200). Dotted lines are only guides to the eyes. The dashed, dotted-dashed, and solid curves are the analytical prediction for $J/D = 0.20$, 0.30 , and 0.50 , respectively, based on Eqs. (21) and (22) and taking into account the finite values of E_c and Δ . The analytical curves were plotted only within their region of validity. The same horizontal scale is used in (a), (b), and (c).

Furthermore, when deriving Eq. (31) we assumed a flat density of states (i.e., a parabolic dispersion relation), which is a rough approximation. Thus, taking into account such limitations, g has to be considered merely as a convenient way to parametrize the transition from a metallic ($g \gg 1$) to a strongly disordered, localized regime ($g < 1$). It is important to remark that g is not equal to the dimensionless conductance parameter $\mathcal{G} \equiv E_c/\Delta$.

A. Average and standard deviation of T_K

The dependence on g of the average and standard deviation of the Kondo temperature, as well as their ratio, is shown in

Fig. 2 for several values of the exchange coupling J . The solid, dashed, and dotted-dashed curves are the analytical predictions for a 20×20 (two-dimensional) lattice based on Eqs. (21) and (22) and taking into account the finite values of E_c and Δ . The clean-limit value of the Kondo temperature, $T_K^{(0)}$, was obtained from Eq. (B1) with the proper adjustment for the Fermi level position.

Figure 2 contains several important features. First, the plots show that the statistics of T_K is quite independent of lattice size and geometry. Even wires with an aspect ratio of 1:25 still present statistical fluctuations of T_K consistent with a two-dimensional geometry after the appropriate rescaling. Deviations are only apparent for the largest value of g considered. This behavior can be understood if we recall that for diffusive dynamics the crossover from 2D to the Q1D regime occurs when the elastic mean free path becomes larger than the wire width but remains smaller than the wire length ($L_y < l < L_x$). For a square lattice with weak site disorder ($g \gg 1$), assuming a flat density of states, it is straightforward to show that

$$\frac{l}{a} \approx g \sqrt{\frac{D}{2E_F}}.$$

Applying this expression to the 10×100 and 8×200 lattices we find that the 2D-Q1D crossover happens around $g = g_c \approx 7$ and 6, respectively. Thus, at $g < g_c$, the electronic eigenstates should follow the statistics of a two-dimensional disordered lattice, irrespective of the wire aspect ratio, and this is indeed what we observe. At $g < 1$, all states are localized and therefore the statistics of T_K becomes independent of lattice size, geometry, or boundary conditions.

In order to reach a regime where the analytical expressions for Q1D [Eqs. (27) and (28)] are applicable, we would need narrower wires or much weaker disorder. At the same time, we would need to maintain a large number of transversal modes and longitudinal diffusion. In practice, these constraints can only be satisfied for much larger lattices than those we have investigated.

It is also clear from Fig. 2 that the average Kondo temperature is only substantially affected by disorder when localization sets in ($g \rightarrow 1$). This behavior is reminiscent of the independence of the critical temperature on nonmagnetic disorder in weakly disordered conventional superconductors.³² In the weak-disorder regime, $\langle T_K \rangle$ follows closely the bulk clean case value of the Kondo temperature [see Eq. (B1)], which is consistent with the prediction of Eq. (21). Deviations only become large in the strong disordered regime, where the analytical expressions are not expected to be valid. The situation is less satisfactory for δT_K , where the deviations from the analytical curves are seen for all disorder strengths. Note that the agreement with Eq. (22) is better for large values of J/D .

Overall, the analytical expressions do capture the qualitative aspects correctly. There is an enhancement of the Kondo temperature and an increase of its variance as the disorder strength increases and g decreases. According to the analytical calculations, this is mainly due to the appearance of weak correlations of wave functions at different energies.

B. The distribution of T_K

The effect of disorder is much more drastic for the distribution of Kondo temperatures as a whole. In Ref. 10, it was found that a bimodal structure appears even for weak disorder and large exchange coupling. To further investigate this effect and its dependence on sample geometry, we present in Fig. 3 the distribution of T_K obtained from numerical calculations involving 10×100 and 8×200 lattices. These should be compared with Fig. 2 in Ref. 10, where the 20×20 case was considered.

Two distinct peaks are clearly visible when J/D is not too small. As J/D increases, weight is transferred from the low- T_K to the high- T_K peak. The distributions never come as close to a Gaussian as they do in the RMT case (see Ref. 10 for the RMT distributions). The distinct features of the distributions are a wide plateau in $P(T_K)$ for weak disorder and a marked second peak at small T_K for strong disorder. Since Eq. (19) indicates that the enhancement of fluctuations in the Kondo temperature survive the thermodynamic limit, we believe that the overall form observed in Fig. 3 should persist as the linear size of the lattice is increased. However, to verify this conjecture, one would need to perform a finite-size scaling analysis over a much wider range of lattice sizes. For an analytical proof, at least a few moments higher than the variance would have to be calculated. Both are beyond the scope of this paper. The finite-size rescaling will be investigated in a future work using a more refined numerical technique.¹¹

It is important to remark that a finite-size scaling analysis was performed in Ref. 29 in the *strong disorder* limit only. It was found that a critical feature seen in Figs. 3(c)-(f), namely, the divergence of the distribution as $T_K \rightarrow 0$ at strong disorder, does survive finite-size scaling. In Ref. 29, this divergence was found numerically to be a power law and it was argued that the exponent depended solely on the lattice space dimension. However, no analytical derivation was given to justify such a behavior. This issue is addressed in Sec. V.

V. DISTRIBUTION OF T_K IN THE LOCALIZED REGIME

For the purpose of investigating the power-law behavior reported in Ref. 29, let us consider the localized regime in more detail. When the localization lengths ξ_n of all states within the energy band are smaller than the system size, one can calculate the distribution function analytically by noting that only states which are located within a distance smaller than ξ_n to the magnetic impurity state contribute significantly to the Kondo screening. The probability density of the n th eigenstate at the position of the magnetic impurity, $\mathbf{r}_0 = 0$, is then given by $(L/\xi_n)^d \exp(-2|\mathbf{r}|/\xi_n)$. We can then average over the center-of-mass positions \mathbf{r}_n of the states closest in energy to the Fermi level. Note that localized states can overlap. When the localization length is sufficiently large, several states can be found within a localization volume ξ^d and the corresponding energy levels will obey Wigner-Dyson statistics. In particular, the two energy levels closest to the Fermi energy repel each other on the scale $\Delta_\xi = 1/(\nu\xi^d)$.

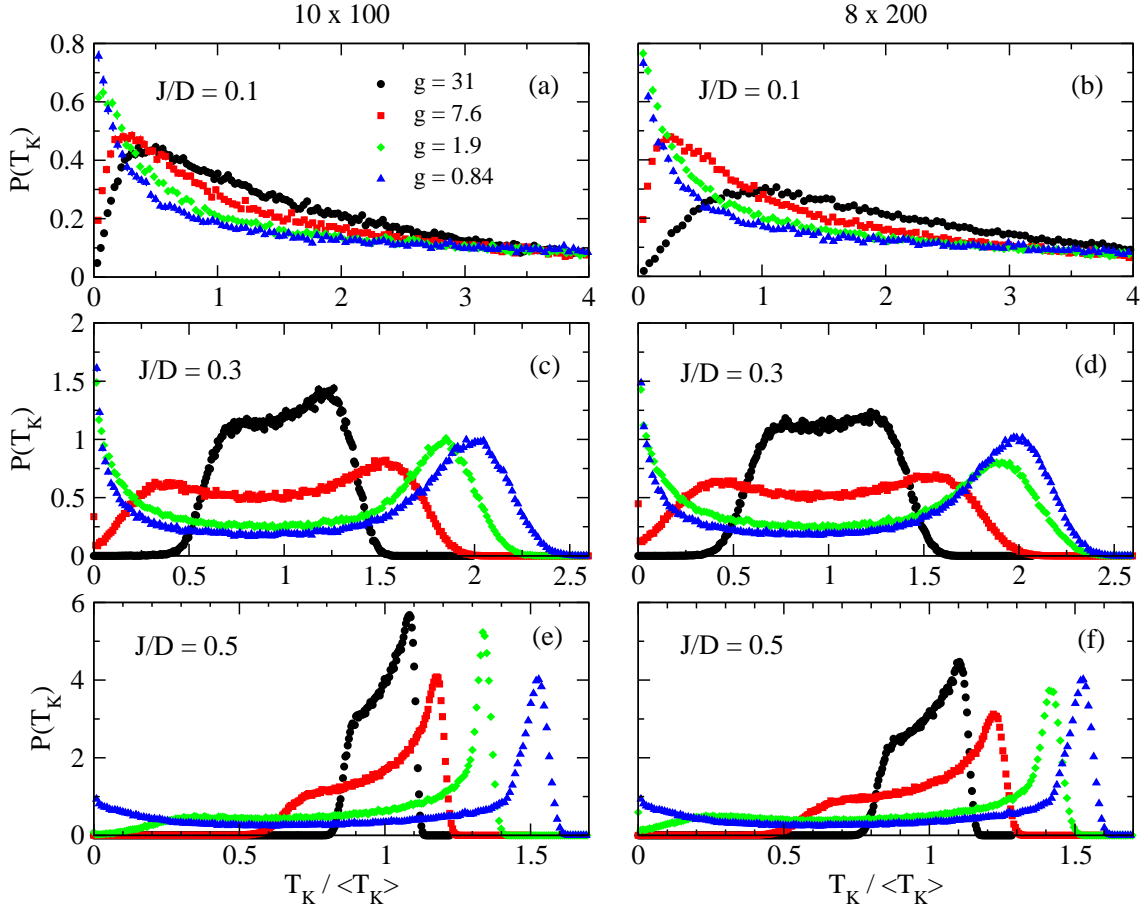


FIG. 3: (Color on-line) The distribution of the Kondo temperatures for 10×100 and 8×200 lattices for a range of disorder strengths and three different values of J/D . Events corresponding to $T_K = 0$ fall outside the vertical scale in (a) and (b).

Under these assumptions, we can use Eq. (3) to derive a distribution of Kondo temperature in the localized regime, namely,

$$P(T_K) = \frac{\Omega}{T_K} \langle F(\epsilon/T_K) \rangle_\epsilon, \quad (33)$$

where Ω is the sample volume,

$$F(x) = \frac{x}{\tanh(x/2) \cosh^2(x/2)} \ln^{d-1} \left[\frac{x T_K}{\Delta_\xi \tanh(x/2)} \frac{D}{J} \right], \quad (34)$$

and $\langle \dots \rangle_\epsilon$ denotes the average over the level spacing ϵ between the states within the localization volume ξ^d which are close to the Fermi energy E_F . Let us now look at both “weak” and “strong” localization regimes.

For large localization lengths, Δ_ξ is much smaller than the bandwidth and we can assume that energy levels in the vicinity of the magnetic impurity repel within the energy window Δ_ξ . As a result, for Kondo temperatures exceeding the local level spacing, $T_K > \Delta_\xi$, the distribution becomes

$$P(T_K) |_{T_K > \Delta_\xi} \sim \frac{\Omega}{T_K} \ln^{d-1} \left(\frac{T_K}{\Delta_\xi} \right), \quad (35)$$

which indeed contains a power law divergence at small T_K but with an exponent independent of the space dimension. As T_K

becomes smaller than Δ_ξ , this divergence is cutoff due to level repulsion. For a fixed level spacing $\epsilon = \Delta_\xi$, one gets an exponential cutoff $P(T_K) |_{T_K < \Delta_\xi} \sim (\Delta_\xi/T_K^2) \exp(-\Delta_\xi/T_K)$. However, the spacing ϵ is known to follow the Wigner surmise, $P(s = \epsilon/\Delta_\xi) = a_\beta s^\beta \exp(-c_\beta s^2)$, where, $a_\beta = \pi/2$ ($32/\pi$) and $c_\beta = \pi/4$ ($4/\pi$), for $\beta = 1$ (2). Performing the average over ϵ , we arrive at

$$P(T_K) |_{T_K < \Delta_\xi} \sim \frac{\Omega a_\beta}{\beta + 2} \frac{T_K^\beta}{\Delta_\xi^{\beta+1}}. \quad (36)$$

This distribution decays (rather than diverge) for $T_K < \Delta_\xi$.

In the strongly localized regime, $g \ll 1$, ξ becomes of the order of the Fermi wave length λ_F . Then, only a single energy level has appreciable overlap with the magnetic impurity. The spacing between the energy level and the Fermi energy obeys a Poissonian distribution, $P(\epsilon) = \exp(-|\epsilon/\Delta_\xi|)$. Averaging over ϵ yields

$$P(T_K) |_{T_K > \Delta_\xi} \sim \frac{1}{T_K} \ln^{d-1} \left(\frac{T_K}{\Delta_\xi} \right) \quad (37)$$

and

$$P(T_K) |_{T_K < \Delta_\xi} \sim \frac{\Delta_\xi/T_K^2}{(2 + \Delta_\xi/T_K)^2} \ln^{d-1} \left(\frac{D}{J} \right). \quad (38)$$

Thus, we also find a power law increase of $P(T_K)$ with decreasing T_K in the strong-disorder limit. But this divergence is also cutoff at $T_K < \Delta_\xi$ and $P(T_K)$ converges to a finite value: $P(T_K) |_{T_K \ll \Delta_\xi} \rightarrow 1/\Delta_\xi$.

In summary, in contrast with the interpretation of the numerical scaling results in Ref. (29), we find that the power of the divergence of $P(T_K)$ does not depend on space dimension, but is rather equal to 1. However, in both cases, the divergence is cut off at $T_K < \Delta_\xi$: For $\xi \gg \lambda_F$, there is a power-law decay, $P(T_K) \sim T_K^\beta$, while for $\xi \rightarrow \lambda_F$ it approaches a constant value, $P(T_K) |_{T_K \ll \Delta_\xi} \rightarrow 1/\Delta_\xi$. These analytical results are found to be in qualitative agreement with our numerical results [see Fig. 3].

It should be noted that while the events corresponding to $T_K = 0$ are not always shown in Fig. 3, they were taken into account in the evaluation of $\langle T_K \rangle$ and δT_K in Figs. 2. The long tail toward the small- T_K region indicates that disorder enhances the probability of having unscreened, free magnetic moments at zero temperature. This is in agreement with the data present in Fig. 4 of Ref. 10, where the probability of finding no solution to Eq. (1) was plotted as a function of J/D .

VI. DISORDERED GRAINS: RANDOM MATRIX THEORY

In a small, weakly disordered, phase-coherent metallic sample, such as a metal grain or nanoparticle,³³ the single-particle energy levels repel each other and the wave function intensities are distributed randomly. This behavior becomes very relevant to several physical properties of the system at low temperatures, namely, when $T < E_c$ (see Fig. 1). This in turn will affect the Kondo temperature associate to magnetic impurities located inside the sample.

For weak disorder, the dimensionless conductance parameter is very large: $\mathcal{G} = E_c/\Delta \rightarrow \infty$. In this regime, the spacing between consecutive levels within a window of energy $\omega < E_c$ obeys the Wigner-Dyson distribution of RMT.³⁴ Moreover, within a given symmetry class, the wave function intensities x_n and the rescaled eigenenergies s_n fluctuate independently. The quantities x_n , $n = 1, \dots, N$, are themselves uncorrelated and obey the so-called Porter-Thomas distributions.^{22,25} For the Gaussian unitary ensemble (GUE - broken time-reversal symmetry class) and for the Gaussian orthogonal ensemble (GOE - time-reversal symmetric class) these distributions are given by

$$P(x_n) = \begin{cases} e^{-x_n}, & \text{GOE,} \\ e^{-x_n/2}/\sqrt{2\pi x_n}, & \text{GUE.} \end{cases} \quad (39)$$

In order to gain insight about the statistical properties of T_K over a wide range of values for J , we have solved Eq. (2) numerically using eigenenergies s_n obtained by diagonalizing GOE and GUE random matrices of size $N = 500$. The resulting semi-circular spectrum was unfolded into a flat band following standard procedures and the Fermi energy was set to the middle of the band ($E_F = 0$). Instead of using the random matrix eigenfunctions to get the local wave function intensi-

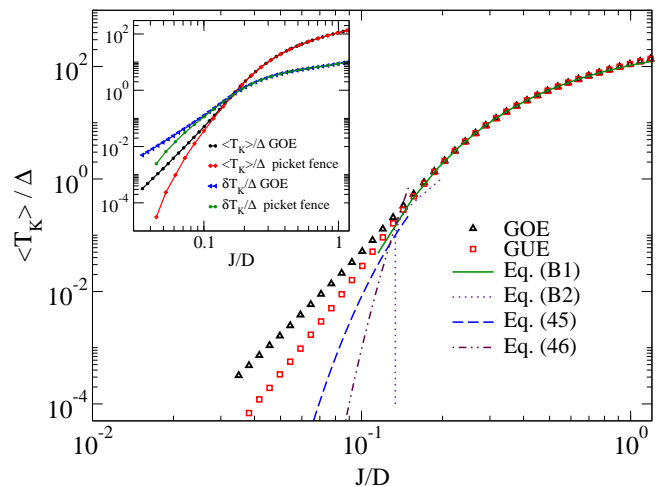


FIG. 4: (Color on-line) The dependence of average Kondo temperature on the exchange coupling for the GOE and GUE compared with the analytical solution in the clean case. Nonzero values of T_K are found below the clean-case threshold given by Eq. (B2) ($J_- \approx 0.134$ here). In this region, T_K is controlled by a few levels close to the Fermi energy, as a comparison with the results of the 2LS model, Eqs. (45) and (46), indicates. Inset: The dependence of the Kondo temperature average $\langle T_K \rangle$ and standard deviation δT_K on the exchange coupling J for unfolded GOE spectra as compared with those obtained for a spectrum of equally spaced energy levels (picket fence). In both cases wave function intensities were drawn from the GOE Porter-Thomas distribution. It is only for $\langle T_K \rangle < \Delta$ that the fluctuations of the energy levels result in an appreciable enhancement of $\langle T_K \rangle$ and δT_K .

ties x_n , we generated these quantities directly from the Porter-Thomas distributions as given in Eq. (39).³⁵ A total of 500 random matrix realizations were used for each ensemble type. For each realization (energy spectrum), we simulated different impurity locations by drawing 250 values of x_n , thereby increasing substantially the statistics of T_K without having to perform a large number of matrix diagonalizations. In Ref. 10, the distribution of Kondo temperatures obtained in this way were shown for several values of J/D . Here we provide a detailed analysis of these and other numerical and analytical results.

In Fig. 4, the GOE and GUE values of $\langle T_K \rangle$ are plotted versus J together with the curves obtained in the clean, thermodynamic limit, namely, Eqs. (B1) and (B3). The average Kondo temperature is found to coincide with the clean case regardless of the ensemble symmetry when $\langle T_K \rangle > \Delta$. It is only for $\langle T_K \rangle < \Delta$ that it becomes dependent on the symmetry class. Note that spectral fluctuations allows for solutions of Eq. (2) below the clean-limit threshold value J_- (see Appendix B). We will return to this point in Sec. VIB.

A. Fluctuations in the large- T_K limit ($T_K > \Delta$)

The average and the standard deviation of the Kondo temperatures for GOE are shown in the inset of Fig. 4. They are compared with results obtained for an equally spaced spec-

trum (picket fence) where the eigenfunction intensities were also drawn from the GOE Porter-Thomas distribution. It is clear that the average and standard deviation of the Kondo temperature are insensitive to level fluctuations when T_K is larger than Δ . We can use this fact to obtain an approximate expression for the distribution of T_K in the RMT: Using Eq. (39) and substituting the delta function by its Fourier integral representation, we can perform the average over the wave function amplitudes in Eq. (3) exactly. For the orthogonal class, assuming an equally spaced spectrum, we obtain

$$P_{\text{GOE}}(T_K) = \left| \frac{d}{dT_K} \sum_{r=1}^{N/2} \exp\left(-\frac{DG_r}{J}\right) \prod_{n=1, n \neq r}^{N/2} \frac{G_n}{G_r - G_n} \right|, \quad (40)$$

where,

$$G_n = (n - 1/2) \coth\left(\frac{n - 1/2}{2\kappa}\right). \quad (41)$$

Equation (40) can only be further simplified in some limiting cases, as outline below.

For $T_K \gg \Delta$, one can set $G_r = r - 1/2$ for $r > \kappa$ and $G_r = 0$ for $r < \kappa$. The Kondo distribution then gains a stretched exponential form,¹⁰

$$P_\beta(T_K) \sim \frac{1}{\Delta} \exp\left[\beta\kappa \ln\left(\frac{e\kappa_0}{\kappa}\right) - \beta\kappa_0\right], \quad (42)$$

where $\kappa_0 = T_K^{(0)}/\Delta$. Note that in the vicinity of $T_K^{(0)}$ the distribution is close to a Gaussian: Near $T_K^{(0)}$ and for $\kappa_0 \gg 1$ it can be approximated as

$$P_\beta(T_K) \sim \frac{1}{\Delta} \exp\left[-\beta(\kappa - \kappa_0)^2/2\kappa_0\right]. \quad (43)$$

The departure from the Gaussian behavior occurs at the tails of the distribution: For $\kappa \ll \kappa_0$ ($\kappa \gg \kappa_0$) the curve defined by Eq. (42) runs below (above) a Gaussian. In Ref. 10, it was noted that $P(T_K)$ becomes wider than Gaussian for small exchange couplings. Even for larger J , when the average $\langle T_K \rangle$ exceeds Δ , clear deviations from the Gaussian behavior were found, with the distribution showing asymmetric non-Gaussian tails. There was good quantitative agreement between Eq. (42) and the numerical data where $\kappa_0 > 1$ and $J < D$.

Using the Gaussian approximation of Eq. (43), we can establish a relation between the standard deviation and the average of the Kondo temperature in the limit $T_K \gg \Delta$, namely,^{10,28,36}

$$\delta T_K |_\beta \approx \sqrt{\frac{\langle T_K \rangle \Delta}{\beta}}, \quad (44)$$

where $\langle T_K \rangle \approx T_K^{(0)}$ is assumed. Since $\langle T_K \rangle$ is ensemble independent in the $T_K \gg \Delta$ limit, one finds from Eq. (44) that $\delta T_{K \text{ GOE}}/\delta T_{K \text{ GUE}} = 1/\sqrt{2}$. These results are compared to the numerical data in Fig. 5. In general, when time-reversal symmetry is present ($\beta = 1$), level repulsion is weaker and the

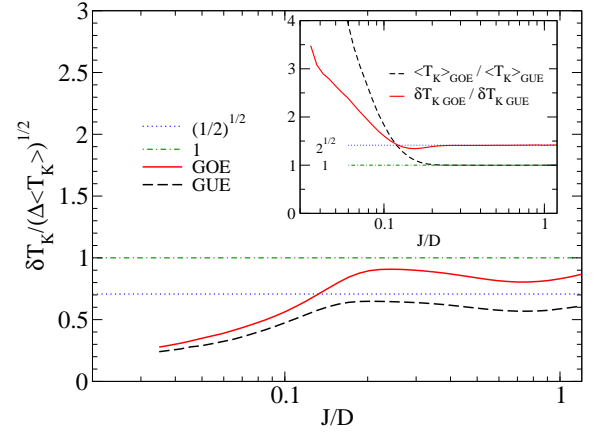


FIG. 5: (Color on-line) The ratio $\delta T_K / (\Delta \langle T_K \rangle)^{1/2}$ as a function of the exchange coupling constant J for the GOE and GUE ensembles. Inset: The ratio between GOE and GUE values for $\langle T_K \rangle$ and δT_K . Analytical considerations predict these ratios to yield the universal numbers 1 and $\sqrt{2}$, respectively, over a wide range of exchange couplings $J > J_-$. Deviations from this behavior are only seen for small exchange couplings, when $J < J_-$. These can be attributed to fluctuations of the two levels closest to the Fermi energy.

tendency to localization stronger. Consequently, the probability of having a vanishing wave function at the magnetic impurity position is enhanced, as well as the probability of large wave function splashes. This indicates that the RMT distribution of T_K should be wider in this case than for the unitary class (broken time-reversal symmetry), in agreement with the results of Ref. 10. The inset of Fig. 5 shows that, where applicable, the analytical prediction for the *ratio* between the standard deviations of the Kondo temperature for the orthogonal and unitary ensembles is in quite good agreement with the numerical results. For both RMT ensembles the distribution width scales with $\sqrt{\Delta}$ and therefore vanishes in the infinite volume limit. In Sec. III we showed that this is no longer true when spectral correlations beyond the Thouless energy scale exist.

There are realizations where no solution with $T_K > 0$ can be found for Eq. (2). They can be interpreted as the absence of screening of the magnetic impurity dipole moment. For a clean system, one can estimate the minimum exchange coupling J_- where Eq. (2) ceases to provide a finite value for T_K (see Appendix B). Non-magnetic disorder strongly affects J_- . For small exchange couplings, free moment events amount to a large portion of all events. Their probability is plotted separately in Fig. 6. It is remarkable that even for $J < J_-$, where $\langle T_K \rangle \ll \Delta$, the distribution shows a clear maximum at a finite value of T_K . The distribution (see Ref. 10) decays towards $T_K = 0$ even though there is a large amount of free moments in this case (see Fig. 6). This peculiar behavior can be qualitatively understood by recalling the level repulsion of RMT ensembles and can be quantitatively treated within a two-level model, as outlined in Sec. VI B below.

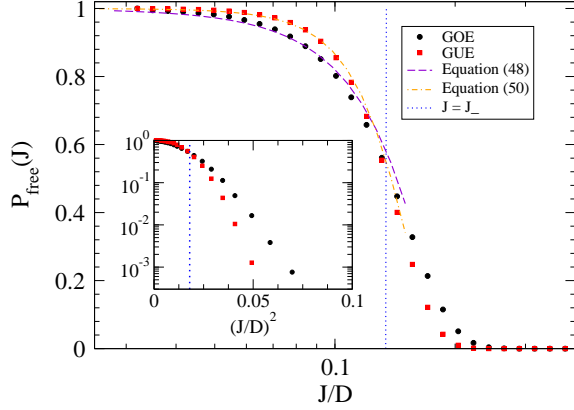


FIG. 6: (Color on-line) Probability of finding free magnetic moments. The data points correspond to the fraction of events in the RMT simulations where either $T_K = 0$ or no solution to Eq. (2) was found, and is plotted as a function of the exchange coupling J . The dotted line indicates the point where $J = J_-$ (clean case threshold). There is a good agreement between simulations and the analytical predictions for $J \ll J_-$ based on the two-level system model. The inset shows the tail of the probability function at $J > J_-$.

B. Two-Level Approximation ($T_K < \Delta$)

For $T_K < \Delta$, only the two states closest in energy to the Fermi energy are appreciably coupled to the magnetic impurity. For small exchange couplings $J < J_-$, this affects the whole distribution of Kondo temperatures, while for larger exchange couplings it applies only to the small- T_K tail. In this limit, we can simplify the analytical calculations by separating the contributions to the sum in Eq. (2) into two groups. In the first we include only the two nearest levels to the Fermi energy and fully take into account the fluctuation of their relative spacing and their wave function amplitudes. The remaining levels form the second group and are treated assuming an equally spaced spectrum and $x_n = 1$. When the wave functions at the Fermi level are distributed according to the GOE Porter-Thomas distribution but the energy levels are kept fixed, the average Kondo temperature is found to be

$$\langle T_K \rangle_{\text{GOE}} = \frac{-\text{Ei}(-1/2)}{2e} \Delta \exp\left(-\frac{D}{J} + \frac{D}{J_-}\right), \quad (45)$$

where $\text{Ei}(x)$ denotes the exponential integral function,³⁷ with $\text{Ei}(-1/2) \approx -0.56$. For the GUE Porter-Thomas distribution, we obtain instead

$$\langle T_K \rangle_{\text{GUE}} = \frac{-2\text{Ei}(-1/2)}{e^2} \Delta \exp\left(-\frac{2D}{J} + \frac{2D}{J_-}\right), \quad (46)$$

showing that the average Kondo temperature in the unitary ensemble becomes exponentially smaller than in the orthogonal ensemble, which is consistent with the numerical result presented in Fig. 5.

It is of particular interest to determine the probability $P_{\text{free}}(J)$ of having unscreened, free magnetic moments in the

system for a given bare exchange coupling. This function is equal to the probability that the Kondo temperature is either zero or that there is no solution to Eq. (2). In these cases, the correction to the exchange coupling remains small for all temperatures and the Kondo effect is quenched, in the sense that the magnetic moment remains unscreened down to zero temperature. As discussed in Appendix B, in the clean limit the free moment probability is a sharp step function of J , namely, $P_{\text{free}}(J \leq J_-) = 1$, and $P_{\text{free}}(J > J_-) = 0$, with J_- given by Eq. (B2). When there is randomness, J_- is a function of the random wave function intensities x_n and level spacings s_n of the closest levels to the Fermi energy. Upon averaging over their distributions, we expect the step function to become a smoothly decaying function. Thus, due to the finite probability that level spacings at the Fermi energy exceed Δ or wave function intensities are small, there is a finite probability of finding free moments even at $J > J_-$, where the magnetic moment would be screened without randomness. We have determined this probability distribution numerically (see Fig. 6). For $J < J_-$, we can compare it with the result obtained within a 2LS approximation. A first attempt can be made by setting the wave function amplitudes to be constant, $x_l = 1$ and fixing all but the two closest levels to the Fermi energy, which are allowed to fluctuate according to the Wigner surmise.³⁴ For the GOE we obtain

$$P_{\text{free}}(J) = \exp\left[-\frac{\pi}{(D/J - D/J_- + 2)^2}\right], \quad (47)$$

which is valid only for $J < J_+ = J_-/(1 - J_-/D)$, since for larger values of J the fluctuations of the other levels can no longer be neglected.

When the wave function amplitudes are constant, the probability to have free magnetic moments is just proportional to the probability that the level spacing at the Fermi energy is of the order of $T_K^{(0)}(J)$. That is exponentially small for $J > J_-$. However, in Fig. 6 we see that the decay with J is slower than that, indicating that the fluctuations of wave functions are crucial. Indeed, under realistic conditions, there is no appealing reason to take $x_l = 1$. When wave functions are allowed to fluctuate according to the Porter-Thomas-distribution, we rather obtain (again for the GOE)

$$\begin{aligned} P_{\text{free}}^{\text{GOE}}(J) &= \int_0^\infty dx \exp\left(-x - \frac{\pi x^2}{4u_J^2}\right) \\ &= u_J \exp\left(\frac{u_J^2}{\pi}\right) \text{Erfc}\left(\frac{u_J}{\sqrt{\pi}}\right), \end{aligned} \quad (48)$$

with

$$u_J = \left|1 + \frac{D}{2J} - \frac{D}{2J_-}\right|. \quad (49)$$

Note that $P_{\text{free}}^{\text{GOE}}(0) = 1$ and $P_{\text{free}}^{\text{GOE}}(J_-) \approx 2/\pi$. For $J > J_-$, the fluctuations of the other energy levels become important and the 2LS approximation can no longer be used. Similarly,

for the GUE we obtain

$$P_{\text{free}}^{\text{GUE}}(J) = 1 - \frac{4}{\pi^2} \int_0^\infty dx x^2 (1 + u_J x) \times \exp\left(-u_J x - \frac{x^2}{\pi}\right). \quad (50)$$

These results are compared to the numerical calculations in Fig. 6 and good agreement is found for $J < J_-$. Thus, in RMT, we can conclude that fluctuations of wave functions do enhance the probability of finding free moments for $J > J_-$.

Finally, there is remarkable feature of the distribution of the Kondo temperature, as shown in Ref. 10, especially noticeable for small exchange couplings ($J/D < 0.1$): Although the number of free moments is large in this regime, the distribution still has a distinct maximum and turns to zero as $T_K \rightarrow 0$. We find that this is due to the energy level repulsion of RMT. Evaluating the distribution function in the 2LS approximation (i.e., for a fixed energy level spacing but fluctuating wave functions), we arrive at $P(T_K) \sim (\Delta/T_K^2)e^{-\Delta/2T_K}$. Then, using the Wigner surmise to average this expression over level spacings, we find that the distribution decays as a power law,

$$P(T_K < \Delta) \sim \frac{a_\beta}{\beta + 2} \frac{T_K^\beta}{\Delta^{\beta+1}}, \quad (51)$$

with $a_1 = \pi/2$ and $a_2 = 32/\pi$, in fair qualitative agreement with the numerical data presented in Ref. 10.

VII. DEPENDENCE OF $P(T_K)$ ON THE CONCENTRATION OF MAGNETIC IMPURITIES

In the absence of an external magnetic field, the symmetry class of the underlying single-particle basis to the Kondo problem is controlled by the concentration of magnetic impurities and the relation between certain energy scales. The general idea is that, as the number of magnetic impurities increases, statistical fluctuations of the electron states in the sample cross over from the orthogonal class (time-reversal symmetric) to the unitary class (broken time-reversal symmetry). This is due to the fact that the spin dynamics of the magnetic impurities can be slow compared to the time scale of the conduction electrons, thereby breaking effectively the time-reversal invariance on their time scale.^{38,39} However, as we will argue below, the dynamical regime in the sample, and consequently the strength of the Kondo screening, also plays a crucial role in determining on which side of this crossover the system finds itself.⁴⁰

We begin by recalling that for a mesoscopic sample in the weak localization (WL) regime, i.e., at energies $E > E_c$ (short time scales), the dimensionless parameter controlling the orthogonal-unitary crossover due to magnetic impurities can be written as³⁸

$$X_s^{\text{WL}} = \frac{1}{E_c \tau_s}, \quad (52)$$

with the crossover centered at $X_s = 1$. As the energy is lowered below E_c (long time scales), one enters the zero-dimensional, RMT regime, where the average level spacing

Δ takes over E_c as the relevant energy scale. In that regime, the crossover parameter is given by

$$X_s^{\text{RMT}} = \frac{1}{\Delta \tau_s} = \mathcal{G} X_s^{\text{WL}} \quad (53)$$

instead. Thus, for a sample in the RMT regime, the crossover occurs for spin scattering rates smaller by a factor $1/\mathcal{G}$ with respect to the weak-localization regime, where \mathcal{G} is the dimensionless conductance. For the RMT regime, this crossover has been recently studied for a Kondo quantum dot in an Aharonov-Bohm ring.⁴¹

At any finite temperature, the spin scattering rate $1/\tau_s$ is renormalized by Kondo correlations: It is small at both $T \gg T_K$ and $T \ll T_K$, having a maximum at around $T = T_K$, as has been observed in weak-localization experiments.^{42,43} This behavior is analogous to that observed in the reentrance of gapless superconductivity.⁴⁴ For a clean sample (see Refs. 30,31),

$$\frac{1}{\tau_s(T)} = \begin{cases} \frac{\pi n_m S(S+1)}{\alpha \frac{n_m}{\pi \nu}} \ln^{-2}(T/T_K), & T > T_K, \\ \frac{n_m}{\pi \nu} \left(\frac{T}{T_K}\right)^2 \frac{w^2 \pi^4}{16} c_{\text{FL}}, & T \ll T_K, \end{cases} \quad (54)$$

where n_m is the density of magnetic impurities, S denotes their spin, α is a numerical factor smaller than unit, and $w \approx 0.41$ is the Wilson number. In Refs. 30 and 31, it was found numerically that $\alpha \approx 0.2$. In Eq. (54), c_{FL} is a factor that arises from the relation between the inelastic scattering rate and the temperature-dependent dephasing rate.³¹ In 2D, $c_{\text{FL}} \approx 0.946$.

A few elucidating remarks about Eq. (54) are in order. First, we define the spin scattering rate as in Ref. 38, which is smaller than the dephasing rate defined in Ref. 31 by a factor $1/2$. Secondly, note the difference between our definition of T_K and that used in Ref. 31: Ours corresponds to their *perturbative* T_K . Thirdly, the numerical prefactor of the $(T/T_K)^2$ term in Eq. (54) was obtained within Fermi liquid theory,¹ where the exact result differs from that obtained in the standard Sommerfeld low-temperature expansion by a factor 3. In the following, we will approximate the numerical prefactor multiplying the $(T/T_K)^2$ term by unit, since $w^2 \pi^4 c_{\text{FL}}/16 = 0.968$.

The low-temperature limit of the spin scattering rate shows the expected Fermi-liquid scaling based on Nozieres' theory for the Kondo problem, which is valid at $T \ll T_K$.^{3,45} At temperatures exceeding T_K , Eq. (54) is consistent with the perturbative poor man's scaling.^{2,21,44,46,47} However, we note that recent experiments have shown the scattering rate to be approximately linear with temperature for a wide interval below T_K .⁴⁸ This behavior has been explained theoretically by Zarand and coworkers using a numerical renormalization group calculation of the frequency-dependent inelastic scattering rate,³⁰ where they also obtained $\alpha \approx 0.2$.

In principle, one could expect that the maximum value $1/\tau_s$ can reach should be given by the unitary limit of the scattering cross section. However, in reality, the maximum value is found to be smaller than that by the factor α shown in Eq.

(54). In 2D,³⁰

$$\frac{1}{\tau_s} \Big|_{\max} = \alpha \frac{n_m}{\pi\nu}, \quad (55)$$

Thus, the maximal value the crossover parameter can reach for a two-dimensional sample in the weak localization regime is

$$X_s^{\text{WL}} \Big|_{\max} = \alpha \frac{N_m}{\pi\mathcal{G}}, \quad (56)$$

where $N_m = n_m L^2$ is the number of magnetic impurities for a sample with linear size L . When there are only a few magnetic impurities, $N_m < \mathcal{G}$, the crossover parameter is small and the sample is in the orthogonal regime. Increasing the concentration of magnetic impurities increases the parameter X_s and eventually leads to the unitary regime. As found in Sec. VI, this is accompanied by a decrease in the width of the distribution of Kondo temperatures.

It has recently been pointed out that the correlations between wave functions at different energies are enhanced in the GOE-GUE crossover regime.¹⁶ Thus, since the width of the distribution of the Kondo temperature is enhanced by wave function correlations, one can expect a widening of the Kondo distribution in the GOE-GUE crossover regime due to the presence of a weak magnetic field or a small amount of spin scattering.⁴⁹ The wave function correlation function is then given by

$$\Omega^2 \langle |\psi_n(\mathbf{r})|^2 |\psi_m(\mathbf{r})|^2 \rangle \Big|_{\omega=E_n-E_m} = \frac{2\lambda^2 \Delta^2}{4\lambda^4 \Delta^2 + \pi^2 \omega^2}, \quad (57)$$

Here, λ is a dimensionless parameter related to the magnitude of the time-reversal breaking perturbation. In the presence of an external magnetic field B , $\lambda^2 = 1/\tau_B \Delta$, where $1/\tau_B$ is the magnetic phase-shift rate. For a diffusive quantum dot, this rate is given by $1/\tau_B = \gamma e^2 D_e B^2 L^2 / \hbar^2$, where γ is a geometrical factor of order unity. In the presence of magnetic impurities, the GOE-GUE crossover is governed by the spin scattering rate and $\lambda^2 = 1/\tau_s \Delta$. Remarkably, the mixing of GOE eigenfunctions brought by time-reversal symmetry breaking induces wave function correlations over a macroscopic energy scale equal to either $1/\tau_B$ or $1/\tau_s$. However, the amplitude of these correlations is proportional to $\tau_s \Delta$ and therefore they vanish in the thermodynamic limit.¹⁶ In order to see that, we use Eq. (12) to explicitly evaluate the width of the distribution of the Kondo temperature related to the crossover wave function correlations. We obtain

$$\langle \delta T_K^2 \rangle = 2 \frac{\Delta}{\tau_s} \int_0^{1/(1+\pi T_K^{(0)} \tau_s)} dt \ln \frac{1+t}{1-t}. \quad (58)$$

Thus, for $T_K^{(0)} \gg 1/\tau_s$, these GOE-GUE correlations only contribute to a width $\delta T_K \approx T_K^{(0)} \sqrt{\tau_s \Delta / \pi}$ that vanishes in the thermodynamic limit when $\Delta \rightarrow 0$, but is larger than the value obtained in the pure RMT ensembles by a factor $\sqrt{T_K^{(0)} \tau_s}$

As the magnetic impurity concentration increases further, the superexchange interaction between magnetic impurities begins to compete with the Kondo screening.⁵⁰ The superexchange interaction coupling J_{RKKY} fluctuates and its average and spreading depend on the amount of disorder, impurity concentration, and details of the Fermi surface. J_{RKKY} is zero on average,⁵¹ but fluctuates according to a wide log-normal distribution.⁵² Its typical value is of the same order as that of a clean sample,⁵³ namely, $\sqrt{\langle J_{\text{RKKY}}^2 \rangle} = (n_m/\nu)(J/D)^2 \cos(2k_F R)$. Even when the typical superexchange coupling constant is smaller than T_K , there is a small chance that clusters of localized spins form. When two localized spins couple ferromagnetically to form a triplet state, they contribute to the dephasing rate of itinerant electrons. Such a contribution to the dephasing rate scales with n_m^2 .^{31,54} When J_{RKKY} exceeds the Kondo temperature T_K of a single magnetic impurity, the spins of the magnetic impurities are quenched. They form a classical random spin array whose spin scattering rate is smaller than that for free quantum spins by the factor $1/3$, and scale linearly with n_m .⁵⁵ At intermediate concentrations of magnetic impurities Griffiths-McCoy singularities can appear and induce an interesting though more complex behavior (see Ref. 56 for a review).

VIII. DEPHASING DUE TO FREE MAGNETIC MOMENTS IN DISORDERED METALS

We now discuss the relevance of the distribution of the Kondo temperature T_K to the quantum corrections of the conductance of mesoscopic wires.

As discussed in Sec. VII [see Eq. (54), in particular], the temperature dependence of the spin scattering rate has a maximum at T_K , resulting in a plateau of the dephasing time.^{42,43} However, we have found in Sec. IV that disorder can result in a finite probability of having magnetic impurities with vanishingly small Kondo temperatures. Thus, the question arises whether the latter effect can yield a finite contribution to the dephasing rate at temperatures below the average Kondo temperature. It has recently been argued that the dephasing rate due to a magnetic impurity can be related to the inelastic cross section of a magnetic impurity at the Fermi energy,^{30,31}

$$\frac{1}{\tau_s} = n_m v_F \sigma_{\text{inel}}, \quad (59)$$

where v_F is the Fermi velocity, and the inelastic cross section can be obtained from the difference between the total and the elastic cross section,

$$\sigma_{\text{inel}}(E_F) = \sigma_{\text{total}} - \sigma_{\text{el}}. \quad (60)$$

Using the optical theorem, both the total and the elastic cross sections can be related to matrix elements of the T -matrix of the magnetic impurity.³⁰ Based on the fact that in the derivation of the weak-localization correction one averages over the disorder potential and thereby recovers translational invariance, the authors of Refs. 30 and 31 calculated the spin scattering rate of Eq. (59) for a plane waves basis. However, one

should calculate the spin scattering rate as averaged over all momentum directions in order to correctly determine how the dephasing rate caused by magnetic impurities is affected by the random environment. Following this approach, we find that the spin scattering rate of a state of energy E should be given by⁵⁷

$$\begin{aligned} 1/\tau_s(E, T) &= \frac{n_m}{\nu} \sum_p \delta(E_p - E) \left[\text{Im} \langle p|T|p \rangle \right. \\ &\quad \left. - \frac{\pi}{\Omega} \sum_{p'} \delta(E_p - E_{p'}) |\langle p|T|p' \rangle|^2 \right]. \end{aligned} \quad (61)$$

Using the relation between the T -matrix element and the propagator of a localized d -level in the Anderson model,³⁰ $G_d(E_n, T)$, we obtain

$$\langle p|T|p' \rangle = -\Omega \psi_{p'}(0) \psi_p^*(0) t_0^2 G_d. \quad (62)$$

Inserting this relation into Eq. (61), we find that the spin scattering rate is given by

$$\begin{aligned} 1/\tau_s(E, T) &= -n_m \Omega \frac{\rho(E, 0)}{\nu} (t_0^2 \text{Im} G_d + \pi \nu t_0^4 G_d^2) \\ &= \frac{\rho(E, 0)}{\nu} 1/\tau_s^{(0)}(E, T), \end{aligned} \quad (63)$$

where $1/\tau_s^{(0)}$ is the inelastic spin scattering rate in a clean system. $1/\tau_s^{(0)}(E, T)$ has a universal dependence on T/T_K , as has been shown in Refs. 30 and 31. Thus, Eq. (63) leads us to conclude that the spin scattering rate not only depends on the ratio T/T_K but also explicitly depends on the local density of states. The same conclusion has been recently reached independently in Ref. (58). But both T_K and $\rho(E, 0)$ are randomly distributed, taking different values for each magnetic impurity, and so will $1/\tau_s(T)$. Note that the distribution of Kondo temperatures alone is not sufficient for determining the average spin scattering rate. We have seen in Sec. III that in a two-dimensional metal, the wave functions correlations at different energies are of order $1/g$. The probability of having simultaneously a small Kondo temperature and a small local density of states at the Fermi energy leading to an anomalous value for the spin scattering rate is thus expected to be of order $1/g$ as well.

We can derive the temperature dependence of the spin scattering rate in a sample with a finite number of magnetic impurities by averaging the dephasing rate of a single magnetic impurity over an ensemble of magnetic impurities. To facilitate the calculations, we approximate the universal function for the dephasing rate by the following function,

$$\begin{aligned} \frac{1}{\tau_s^{(0)}} &= \frac{\pi n_m S(S+1)}{\nu} \left\{ \ln^2 \left(\frac{T}{T_K} \right) \right. \\ &\quad \left. + \pi^2 S(S+1) \left[\left(\frac{T_K}{T} \right)^2 + \frac{1}{\alpha} - 1 \right] \right\}^{-1}, \end{aligned} \quad (64)$$

with $\alpha = 0.2$, as found numerically in Ref. 30. Note that temperature scales with T_K only. Equation (64) coincides with

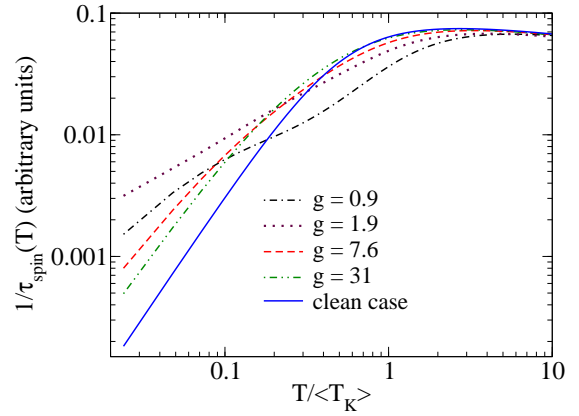


FIG. 7: The spin relaxation rate as a function of temperature for $J/D = 0.24$. The broken lines correspond to ensemble averages of Eq. (63) over fluctuating Kondo temperatures and the LDOS at the Fermi energy (data from the 20×20 lattice simulations was used). The solid line is obtained from Eq. (64) setting $T_K = \langle T_K \rangle$ (clean case).

Eq. (54) in both low- and high-temperature limits. In Fig. 7 we show the result of using Eq. (64) in Eq. (63) and ensemble averaging the spin relaxation rate over T_K and $\rho(E_F, 0)$ obtained numerically for the 20×20 lattice model (see Sec. IV).

One finds a clear departure from the clean case prediction at low temperatures,³¹ which amounts to an enhancement of the spin scattering due to the presence of nonmagnetic disorder. Moreover, the maximum value of the spin scattering rate is found to be reduced in proportion to the disorder strength and its position shifted to larger temperatures. A very similar behavior has been recently observed in weak-localization measurements performed by the Grenoble group on quasi-one-dimensional Ag wires doped with 2 to 20 ppm Fe impurities,⁵⁹ as well as by the Michigan group,⁶⁰ where similar samples were implanted with 2 to 10 ppm of Fe impurities. One should note that these samples have very high diffusion constants, of order $D_e = 300 - 400 \text{ cm}^2/\text{s}$, so that the parameter g in these samples is large, $g > 100$. For the Fermi energy in Ag, $E_F = 5.5 \text{ eV}$, and the Kondo temperature of $T_K = 4 \text{ K}$, the ratio between band width and exchange coupling is found to be of the order of $J/D = 0.1$. Thus, according to Eq. (23), $\delta T_K / \langle T_K \rangle \ll 1$ is fulfilled and the width of the distribution of Kondo temperatures should be negligible in 2D samples. However, one has to be careful when considering the relevance of our results to the weak-localization experiments of Refs. 59 and 60. For instance, we note that the low-temperature dephasing rate is dominated by the non-Gaussian low- T_K tail of the distribution of the Kondo-temperature, which we have found to be present even for weak disorder, $g \gg 10$. Moreover, the samples used in Refs. 59 and 60 were quasi-one-dimensional, in which case δT_K is known to be further enhanced (see Sec. III).

In order to connect theory with experiments, some more work needs to be done. On the theoretical side, a systematic study of how the distribution of the Kondo temperature

scales with the width and length of the sample is necessary. This is the subject of ongoing work and will be published elsewhere.¹¹ On the experimental side, the relevance of the distribution of the Kondo temperature to the low-temperature anomaly of the dephasing rate could be established by utilizing samples with lower diffusion constants, such as the low-mobility samples of AuPd, examined in Ref. 61 (see also Ref. 62). These have diffusion constants as low as $D_e = 13.4 \text{ cm}^2/\text{s}$, corresponding to $g \approx 17$. The presence of free magnetic moments would be facilitated in semiconductors such as Si and GaAs where the effective mass of electrons is smaller than in metals by a factor 30. Moreover, 2D electron gases with $ak_F \approx 1$ can be produced with those materials. In low-mobility GaAs wires, Anderson localization has been observed even in wires with $g \approx 30$.⁶³ Thus, all mesoscopic energy scales can become relevant when the system reaches temperatures of the order of 1 K. However, so far no magnetic impurities with detectable Kondo temperatures have been found in semiconductors, since the low density of states suppresses the Kondo temperature exponentially.

IX. CONCLUSIONS

The screening of magnetic moments in metals, the Kondo effect, is found to be quenched with a finite probability in the presence of nonmagnetic disorder. For weak disorder, $g \gg 1$, the effect is shown analytically and numerically to be due to wave function correlations. Albeit weak in the metallic regime, these correlations have a sizeable effect on the Kondo temperature. That is because the Kondo temperature involves a summation over all eigenstates with a finite wave function amplitude at the location of the magnetic impurity. As disorder increases and the sample goes from the diffusive to the localized regime, an increase in the correlations of the LDOS at different energies induces even stronger fluctuations in the Kondo temperature. Thus, the distribution of the Kondo temperature $P(T_K)$ retains a finite width in the limit of vanishing level spacing Δ . When time-reversal symmetry is broken either by applying a magnetic field or by increasing the concentration of magnetic impurities, $P(T_K)$ becomes narrower. The probability that a magnetic moment remains free down to the lowest temperatures is found to increase with disorder strength. This result is consistent with direct measurements of Kondo effect in Cu(Fe) thin films and Au(Fe) wires.⁶⁴

We have also shown that magnetic impurities with a small Kondo temperature are shown to modify the temperature dependence of the dephasing rate at low temperatures, $T \ll \langle T_K \rangle$, as measured in weak-localization transport experiments.

Equations (20) and (26) allow us to conclude that the disorder can substantially affect the Kondo temperature. This could be contrasted with the effect of disorder on another energy scale derived from a many-body state, namely, the critical temperature of a superconductor, T_c . Anderson's theorem states that T_c is not affected by nonmagnetic disorder.³² Our results demonstrate that there is no analog to this theorem for the Kondo temperature of magnetic impurities embedded in

low-dimensional disordered systems since the variance of T_K depends markedly on the disorder strength. This conclusion, however, is at odds with the proposal of Ref. 65, where it was argued that in the low-temperature, strong coupling limit, the Kondo effect is not affected by disorder at all. We note that this result was obtained using a path integral representation and a semiclassical expansion (the large- N limit is taken, where $N = 2s + 1$ is the number of spin components). The disagreement between Ref. 65 and our results may not be real, however, since their calculation is limited to $T \ll T_K$ and cannot rule out the existence of magnetic impurities with exceedingly small T_K .

It remains to be studied how the distribution of T_K scales with system size and how it changes (if at all) in the quasi-one-dimensional limit. The numerical techniques employed in this work did not permit the investigation of sufficiently large lattices. It also remains to be checked whether the large fluctuations of T_K seen at strong disorder survive a non-perturbative approach such as the numerical renormalization group. Finally, we note that we have not attempted to explore the consequences of having a free magnetic moments to the nature of the electron liquid. This issue has been recently addressed by other authors in the context of heavy-fermion materials.^{9,56}

Acknowledgments

The authors gratefully acknowledge useful discussions with Harold Baranger, Carlo Beenakker, Antonio Castro Neto, Claudio Chamon, Vladimir Dobrosavljevic, Peter Fulde, Ribhu Kaul, Vladimir Kravtsov, Caio Lewenkopf, Alexander Lichtenstein, Ganpathy Murthy, Mikhail Raikh, Achim Rosch, Denis Ullmo, Chandra Varma, Isa Zarekeshev, and Andrey Zhuravlev. The authors thank the hospitality of the Condensed Matter Theory Group at Boston University, where this work was initiated, and the Aspen Center for Physics, where the manuscript was finalized. S.K. also acknowledges the hospitality of the Max-Planck Institute for Physics of Complex Systems and the Department of Physics at the University of Central Florida. E.R.M. thanks the hospitality of the Institute for Theoretical Physics at the University of Hamburg. This research was supported by the German Research Council (DFG) under SFB 508, A9, and SFB 668, B2.

APPENDIX A: DERIVATION OF EQ. (1)

We begin with the Anderson model, namely, a localized d -level coupled to a conduction band,²¹

$$H = \sum_{n,\sigma} E_n \hat{n}_{n\sigma} + \varepsilon_d \sum_{\sigma} \hat{n}_{d\sigma} + U \hat{n}_{d+} \hat{n}_{d-} + \sum_{n,\sigma} (t_{nd} c_{n\sigma}^{\dagger} c_{d\sigma} + t_{dn} c_{d\sigma}^{\dagger} c_{n\sigma}), \quad (\text{A1})$$

where E_n are the eigenenergies of the conduction band electrons, ε_d is the energy of a singly occupied d -level, and $\varepsilon_d + U$ is the energy of a doubly occupied d -level. $t_{dn} = t_{nd}^*$ are

the hybridization matrix elements between the d -level and the conduction band state $|n\rangle$. Projecting out of the Hilbert space all state where the d -levels are doubly occupied one obtains the Kondo Hamiltonian

$$H_J = J \mathbf{s} \cdot \mathbf{S}, \quad (\text{A2})$$

where the matrix elements of the exchange interaction in the basis of the eigenstates of the conduction electrons are given by

$$J_{kl} = \frac{8 t_{kd} t_{dl}}{U}. \quad (\text{A3})$$

These matrix elements are positive and thus the interaction is antiferromagnetic. The hopping matrix element connecting the localized d -state $\phi_d(\mathbf{r})$ to the conduction band state $\psi_n(\mathbf{r})$ is given by

$$t_{dn} = \int d^d r \phi_d^*(\mathbf{r}) V(\hat{\mathbf{r}}) \psi_n(\mathbf{r}), \quad (\text{A4})$$

where \hat{V} is the potential energy of the tunneling barrier. For an impurity state strongly localized at $\mathbf{r} = 0$ we obtain

$$J_{kl} \approx J \phi_d^*(0) \psi_n(0), \quad (\text{A5})$$

where $J = 8(1/m^* a_0^2)^2 U$, m^* is the band mass, and a_0 is the radius of the localized state at the magnetic atom. We define T_K by the divergence of second-order perturbation theory. To second order in J , there are two processes to be considered: (i) The scattering due to the exchange coupling J of an electron from state $|n\rangle$ to a state $|l\rangle$ close to the Fermi energy via an intermediate state $|m\rangle$. This process is proportional to the probability that state $|m\rangle$ is not occupied, $1 - f(E_m)$, where $f(E)$ is the Fermi distribution. (ii) The reverse process, in which a hole is scattered from the state $|l\rangle$ to the state $|n\rangle$ via the occupied of a state $|m\rangle$ with probability proportional to the occupation factor $f(E_m)$. Thus, we find that the exchange coupling is renormalized to

$$\tilde{J}_{nl} = J_{nl} \left[1 + \frac{J}{2N} \sum_m \frac{\Omega |\psi_m(0)|^2}{E_m - E_F} \tanh \left(\frac{E_m - E_F}{2T} \right) \right]. \quad (\text{A6})$$

For positive exchange coupling, $J > 0$, perturbation theory diverges as the temperature is lowered. Defining the Kondo temperature as the temperature where the second-order correction to the exchange coupling becomes equal to the bare coupling, we arrive at Eq. (1).

An equivalent expression can be derived from the renormalization group equation, which in the two-loop approximation is given by²⁷

$$\begin{aligned} \frac{dJ}{dt} = & J^2 \frac{\rho(E_F + \Lambda) + \rho(E_F - \Lambda)}{2D\nu} \\ & - \frac{1}{2} \frac{J^3}{D^2} \frac{\rho(E_F - \Lambda)}{\nu} \int_0^\Lambda \frac{dE}{\Lambda} \frac{\rho(E_F + E)/\nu}{(1 + E/\Lambda)^2} \\ & - \frac{1}{2} \frac{J^3}{D^2} \frac{\rho(E_F + \Lambda)}{\nu} \int_0^\Lambda \frac{dE}{\Lambda} \frac{\rho(E_F - E)/\nu}{(1 + E/\Lambda)^2}, \end{aligned} \quad (\text{A7})$$

where $t = \ln D/(2\Lambda)$. Defining T_K as the value of Λ at which J flows to the band width D and solving Eq. (A7) for T_K , we obtain for a clean system

$$T_K^{(0)2\text{-loop}} = \frac{e}{2^{3/2}} \sqrt{\frac{J}{D}} \exp(-D/J). \quad (\text{A8})$$

However, if we keep only the first term on the right-hand side of Eq. (A7) - the one-loop term, we obtain a self-consistency equation for the Kondo temperature that reads

$$\ln \left[\frac{T_K}{T_K^{(0)}} \right] = \frac{1}{2} \int_{2T_K/D < |t| < 1} \frac{dt}{t} \left[\frac{\delta\rho(E_F + Dt/2)}{\nu} \right] \quad (\text{A9})$$

For $T_K \gg \Delta$, Eq. (A9) coincides with the self-consistency equation obtained using perturbation theory, namely, Eq. (1).

APPENDIX B: CLEAN CASE

We briefly describe the behavior of the Kondo temperature in the clean, bulk limit. For that purpose, we assume a spectrum of N equally spaced levels, band width $D = N\Delta$, and spatially uniform wave function intensities (plane waves). When the Fermi energy is in the middle of the band and N is even, all levels are either doubly occupied or empty at $T = 0$ and we have $s_n = n - N/2 - 1/2$, $n = 1, \dots, N$. For $N \gg 1$ and $T_K \gg \Delta$, we then find for Eq. (1) the well-known solution

$$T_K^{(0)} \approx 0.57 D \exp(-D/J), \quad (\text{B1})$$

which agrees to lowest order in J/D with results from more accurate methods such as the numerical renormalization group. In fact, for the latter, the next leading order correction in the exponent has been found to be $-0.5 \ln(D/J)$,⁴ indicating that our treatment is valid for $J < D$ up to preexponential corrections. For small J , however, T_K approaches Δ and turns abruptly to zero at

$$J_- = \frac{D}{\ln(2N) + C} \quad (\text{B2})$$

in a nonanalytical fashion, namely,

$$T_K^{(0)}(J \rightarrow J_-) = -\frac{\Delta}{2} \frac{1}{\ln[(D/J_- - D/J)/4]} \quad (\text{B3})$$

(here $C \approx 0.58$ is the Euler number). For $J < J_-$, Eq. (1) has no solution in the clean limit. That means that the lowest order corrections to the bare exchange coupling remain weak down to zero temperature and marginal terms have to be included in order to determine T_K .⁴ Nevertheless, $T_K \ll \Delta$ in this regime and we can conclude that there will be unscreened magnetic impurities (free moments) down to the lowest accessible temperatures in bulk clean metals when $J < J_-$.

- ¹ A. C. Hewson, *The Kondo Problem to Heavy Fermions* (Cambridge University Press, 1997).
- ² A. A. Abrikosov, *Fundamentals of the Theory of Metals* (North Holland, Amsterdam, 1988).
- ³ P. Nozières, *J. Low-Temp. Phys.* **17**, 3 (1974).
- ⁴ K. G. Wilson, *Rev. Mod. Phys.* **47**, 773 (1975).
- ⁵ E. Miranda and V. Dobrosavljević, *Rep. Progr. Phys.* **68**, 2337 (2005).
- ⁶ R. N. Bhatt and D. S. Fisher, *Phys. Rev. Lett.* **68**, 3072 (1992).
- ⁷ A. Langenfeld and P. Wölfle, *Ann. Physik* **4**, 43 (1995).
- ⁸ R. K. Kaul, D. Ullmo, and H. U. Baranger, *Phys. Rev. B* **68**, 161305(R) (2003).
- ⁹ E. Miranda, V. Dobrosavljević, and G. Kotliar, *J. Phys. Cond. Mat.* **8**, 9871 (1996).
- ¹⁰ S. Kettemann and E. R. Mucciolo, *Pis'ma v ZhETF*, **83**, 284 (2006) [*JETP Letters* **83**, 240 (2006)].
- ¹¹ A. Zhuravlev, I. Zharekeshv, E. R. Mucciolo, and S. Kettemann, unpublished (2007).
- ¹² B. L. Altshuler and B. I. Shklovskii, *Zh. Eksp. Theor. Fiz.* **91**, 220 (1986) [*Sov. Phys. JETP* **64**, 127 (1986)].
- ¹³ A. G. Aronov, V. E. Kravtsov, and I. V. Lerner, *Phys. Rev. Lett.* **74**, 1174 (1995).
- ¹⁴ A. Altland and D. Fuchs, *Phys. Rev. Lett.* **74**, 4269 (1995).
- ¹⁵ S. Kettemann, *Phys. Rev. B* **59**, 4799 (1999).
- ¹⁶ S. Adam, P. W. Brouwer, J. P. Sethna, and X. Waintal, *Phys. Rev. B* **66**, 165310 (2002); S. Braig, S. Adam, and P. W. Brouwer, *Phys. Rev. B* **68**, 035323 (2003).
- ¹⁷ W. B. Thimm, J. Kroha, and J. von Delft, *Phys. Rev. Lett.* **82**, 2143 (1999).
- ¹⁸ S. Suga and T. Ohashi, *J. Phys. Soc. Jpn.* **72** Suppl. A, 139 (2003).
- ¹⁹ Y. Nagaoka, *Phys. Rev.* **138**, 1112 (1965).
- ²⁰ P. Fulde, *Electron Correlations in Molecules and Solids*, 2nd ed. (Springer, Berlin, 1993).
- ²¹ P. W. Anderson, *Phys. Rev.* **124**, 41 (1961); P. W. Anderson, G. Yuval, and D. R. Hamann, *Phys. Rev. B* **1**, 4464 (1970).
- ²² K. B. Efetov, *Supersymmetry in Disorder and Chaos* (Cambridge University Press, Cambridge, 1997).
- ²³ V. N. Prigodin and K. B. Efetov, *Phys. Rev. Lett.* **70**, 2932 (1993).
- ²⁴ C. W. J. Beenakker, *Phys. Rev. B* **50**, 15170 (1994).
- ²⁵ A. D. Mirlin, *Phys. Rep.* **326**, 259 (2000).
- ²⁶ M. Miller, D. Ullmo, and H. U. Baranger, *Phys. Rev. B* **72**, 045305 (2005).
- ²⁷ G. Zaránd and L. Udvardi, *Phys. Rev. B* **54**, 7606 (1996).
- ²⁸ S. Kettemann, in *Quantum Information and Decoherence in Nanosystems*, eds. D. C. Glattli, M. Sanquer, and J. Tran Thanh Van (The Gioi Publishers, 2004), p.259.
- ²⁹ P. S. Cornaglia, D. R. Grempel, and C. A. Balseiro, *Phys. Rev. Lett.* **96**, 117209 (2006).
- ³⁰ G. Zaránd, L. Borda, J. von Delft, and N. Andrei, *Phys. Rev. Lett.* **93**, 107204 (2004).
- ³¹ T. Micklitz, A. Altland, T. A. Costi, and A. Rosch, *Phys. Rev. Lett.* **96**, 226601 (2006).
- ³² P. W. Anderson, *J. Phys. Chem. Solids* **11**, 26 (1959); A. A. Abrikosov and L. P. Gorkov, *Sov. Phys. JETP* **8**, 1090 (1958).
- ³³ E. R. Mucciolo, C. H. Lewenkopf, and L. I. Glazman, *Phys. Rev. B* **74**, 121402(R) (2006).
- ³⁴ M. L. Mehta, *Random Matrices* (Academic Press, Boston, 1991).
- ³⁵ We did not use the eigenfunctions resulting directly from the diagonalization of the GOE and GUE matrices to compute the Kondo temperature for the following reason. Even though these eigenfunctions do obey the Porter-Thomas distributions individually, they are constrained by the normalization condition $\sum_{n=1}^N x_n = N$. That alone makes $\delta T_K \rightarrow 0$ as J approaches D and T_K itself becomes of order D . While this is correct for a single-band lattice model, it is not adequate for describing a multi-band continuous system.
- ³⁶ R. K. Kaul, D. Ullmo, S. Chandrasekharan, and H. U. Baranger, *Europhys. Lett.* **71**, 973, (2005).
- ³⁷ I. S. Gradshteyn and I. M. Ryzhik, *Table of Integrals, Series, and Products* (Academic Press, San Diego, 1992).
- ³⁸ S. Hikami, A. I. Larkin, and Y. Nagaoka, *Prog. Theor. Phys.* **63**, 707 (1980).
- ³⁹ A. A. Bobkov, V. I. Fal'ko, and D. E. Khmel'nitskii, *Sov. Phys. JETP* **71**, 393 (1990) [*Zh. Eksp. Teor. Fiz.* **98**, 703 (1990)].
- ⁴⁰ S. Kettemann and M. E. Raikh, *Phys. Rev. Lett.* **90**, 146601 (2003).
- ⁴¹ C. H. Lewenkopf and H. A. Weidenmüller, *Phys. Rev. B* **71**, 121309(R) (2005).
- ⁴² G. Bergmann, *Phys. Rev. Lett.* **58**, 1236 (1987); R. P. Peters, G. Bergmann, and R. M. Mueller, *ibid.* **58**, 1964 (1987); C. Van Haendonck, J. Vranken, and Y. Bruynseraede, *ibid.* **58**, 1968 (1987).
- ⁴³ P. Mohanty and R. A. Webb, *Phys. Rev. Lett.* **84**, 4481 (2000).
- ⁴⁴ M. B. Maple, in *Magnetism*, edited by H. Suhl (Academic, New York, 1973), Vol. 5, p. 289.
- ⁴⁵ I. Affleck and A. W. W. Ludwig, *Phys. Rev. B* **48**, 7297 (1993).
- ⁴⁶ E. Müller-Hartmann and J. Zittartz, *Phys. Rev. Lett.* **26**, 428 (1971).
- ⁴⁷ H. Suhl, *Phys. Rev. A* **138**, 515 (1965).
- ⁴⁸ F. Schopfer, C. Bäuerle, W. Rabaud, and L. Saminadayar, *Phys. Rev. Lett.* **90**, 056801(2003).
- ⁴⁹ V. E. Kravtsov, private communication.
- ⁵⁰ M. A. Ruderman and C. Kittel, *Phys. Rev.* **96**, 99 (1954); T. Kasuya, *Prog. Theor. Phys.* **16**, 45 (1956); K. Yosida, *Phys. Rev.* **106**, 893 (1957).
- ⁵¹ P. G. de Gennes, *J. Phys. Radium* **23**, 630 (1962).
- ⁵² I. V. Lerner, *Phys. Rev. B* **48**, 9462 (1993).
- ⁵³ A. Yu. Zyuzin and B. Z. Spivak, *Pis'ma Zh. Eksp. Teor. Fiz.* **43**, 185 (1986) [*JETP Lett.* **43**, 234 (1986)].
- ⁵⁴ G. Frossati, J. L. Tholence, D. Thoulouze, and R. Tournier, *Physica B* **84**, 33 (1976).
- ⁵⁵ W. Wei, G. Bergmann, and R. P. Peters, *Phys. Rev. B* **38**, 11751 (1988).
- ⁵⁶ A. H. Castro Neto and B. A. Jones, *Phys. Rev. B* **62**, 14975 (2000).
- ⁵⁷ Note that the spin scattering rate in Eq. (61) is 1/2 of the dephasing rate as defined in Ref. 31.
- ⁵⁸ T. Micklitz, T. A. Costi, A. Rosch, *cond-mat/0610304*.
- ⁵⁹ F. Mallet, J. Ericsson, D. Mailly, S. Unlubayir, D. Reuter, A. Melnikov, A.D. Wieck, T. Micklitz, A. Rosch, T. A. Costi, L. Saminadayar, and C. Bauerle, *Phys. Rev. Lett.* **97**, 226804 (2006).
- ⁶⁰ G. M. Alzoubi and N. O. Birge, *Phys. Rev. Lett.* **97**, 226803 (2006).
- ⁶¹ A. Trionfi, S. Lee, and D. Natelson, *Phys. Rev. B* **70**, 041304(R) (2004).
- ⁶² J. J. Lin and N. Giordano, *Phys. Rev. B* **35**, 1071 (1987).
- ⁶³ M. E. Gershenson, Yu. B. Khavin, A. G. Mikhalechuk, H. M. Bözler, and A. L. Bogdanov, *Phys. Rev. Lett.* **79**, 725 (1997).
- ⁶⁴ J. J. Lin and N. Giordano, *Phys. Rev. B* **35**, 1071 (1987); M. A. Blachly and N. Giordano, *ibid.* **46**, 2951 (1992).
- ⁶⁵ S. Chakravarty and C. Nayak, *Int. J. Mod. Phys. B* **14**, 1421 (2000).